From Diffraction to Scattering Holography

A Lausi

Sincrotrone Trieste, S.S. 14 - Km 163.5, Area Science Park, 34012 Basovizza - Trieste, ITALY

Elettra
Sincrotrone
Trieste

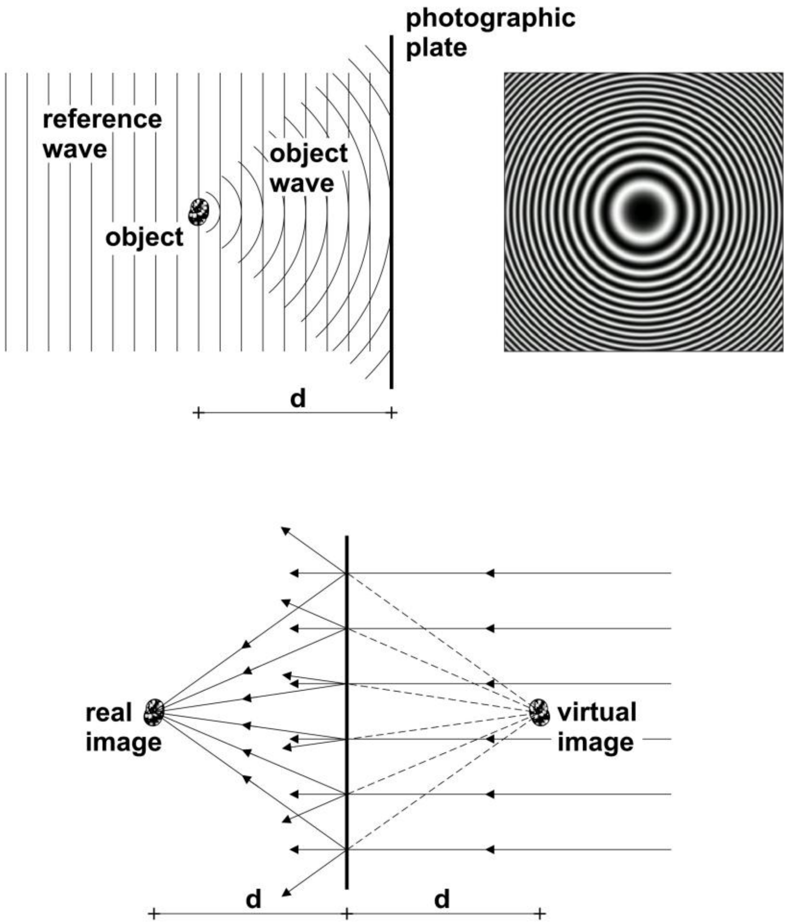

Gabor (in-line) holography

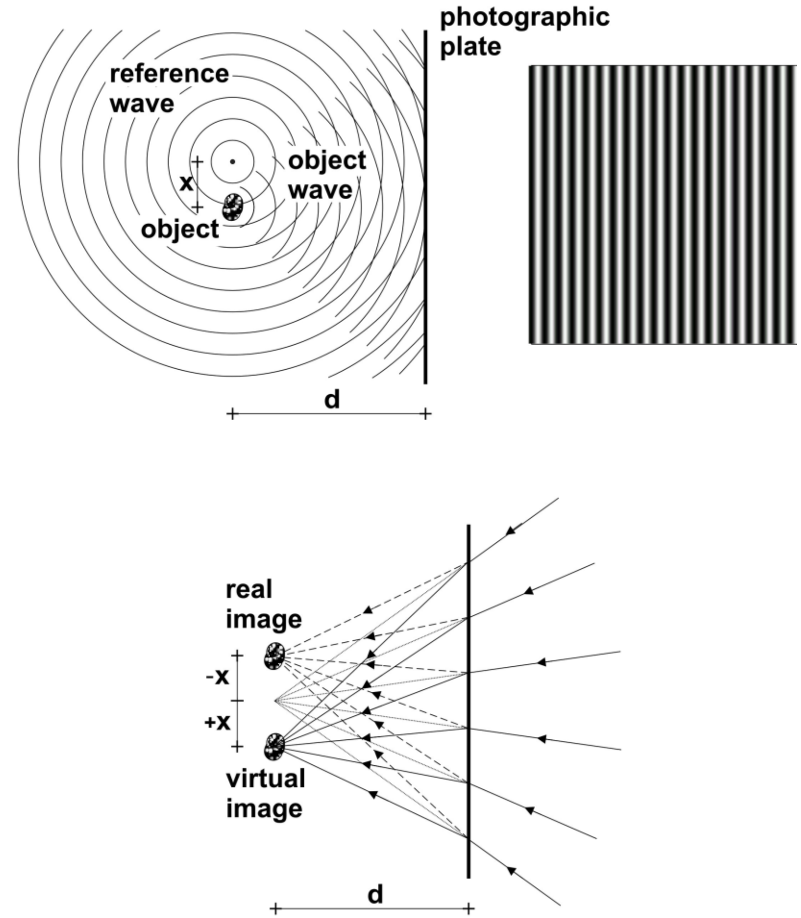

Fourier holography

XFH – Timeline Milestones

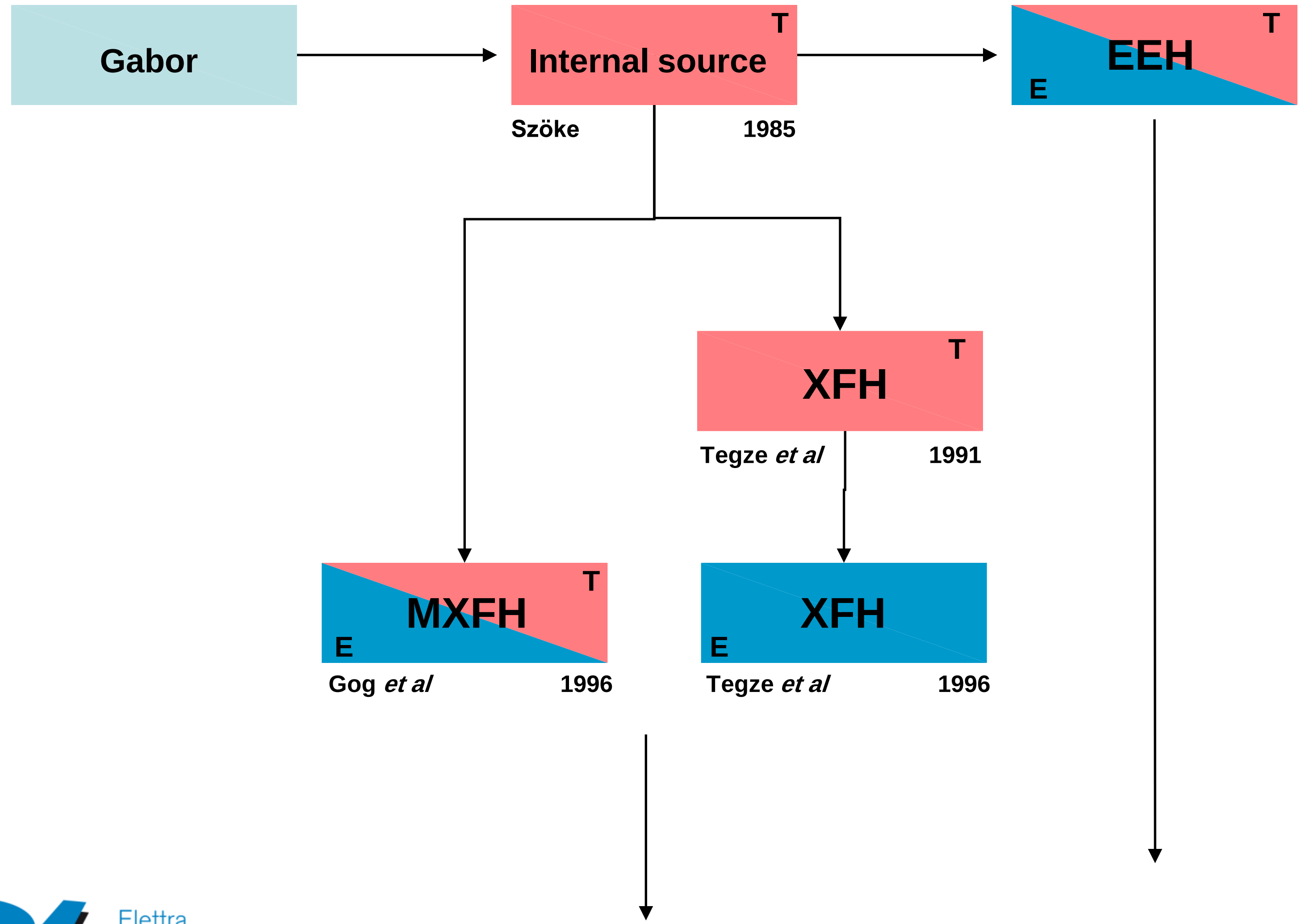

Elettra
Sincrotrone
Trieste

XFH – the internal source scheme

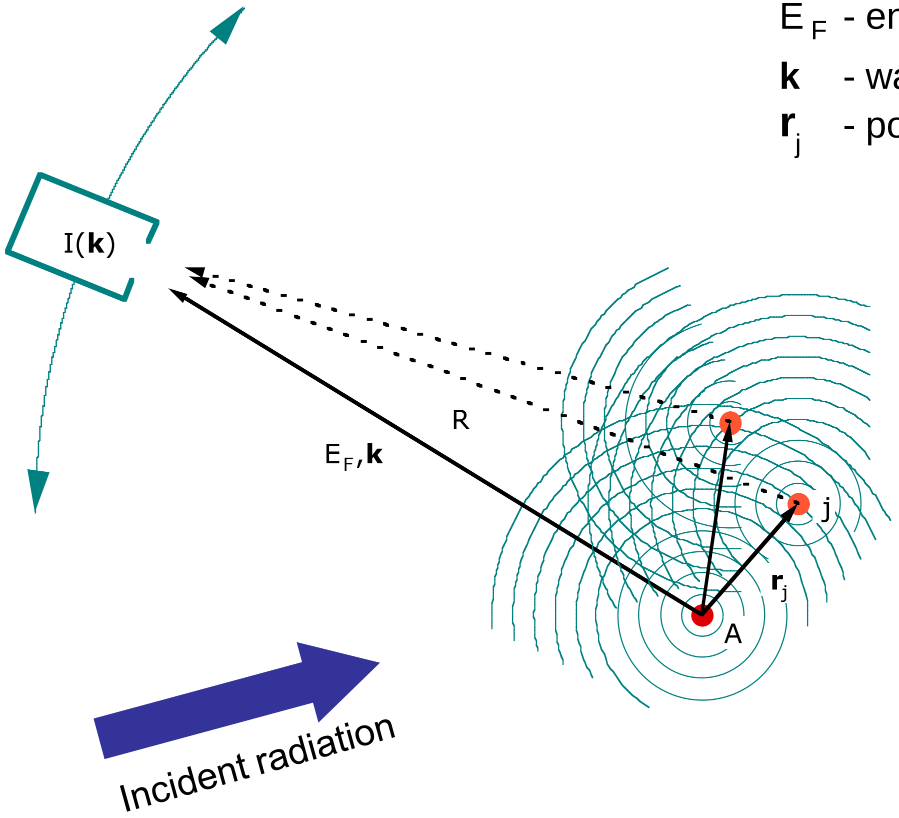

A - reference atom

R - sample - to - detector distance

E_F - energy of x-ray fluorescence from A

k - wave vector

$\mathbf{r}_j$ - position vector of j-th atom

A. Szöke, AIP Conf. Proc. 147, 361 (1986)

Wave function

$$\psi_{tot}(\mathbf{k}) = \psi_0(\mathbf{k}) + \psi_S(\mathbf{k}, \mathbf{r}_j)$$

Reference wave: $$\psi_0(\mathbf{k}) = \frac{e^{ikR}}{R}$$

Object waves: $$\psi_S(\mathbf{k}, \mathbf{r}_j) = \sum_j \frac{e^{ikr_j}}{r_j} f(\mathbf{k}.\mathbf{r}_j) \frac{e^{i(kR - \mathbf{k}.\mathbf{r}_j)}}{R - \mathbf{k}.\mathbf{r}_j / k}$$

$$\left| f(\mathbf{k}.\mathbf{r}_j) \right| \cong Z r_c \cos 2\theta$$

$r_c = 2.82 \times 10^{-15}\,\mathrm{m}$	classical electron radius
Z	atomic number
2θ	diffraction angle

XFH – theoretical background

Intensity

$$I(\mathbf{k}) = |\psi_{tot}(\mathbf{k})|^2 = |\psi_0(\mathbf{k})|^2 + |\psi_S(\mathbf{k},\mathbf{r}_j)|^2 + \\ + \psi_0(\mathbf{k})\psi_S^*(\mathbf{k},\mathbf{r}_j) + \psi_0^*(\mathbf{k})\psi_S(\mathbf{k},\mathbf{r}_j)$$

intensity of the reference wave:

$$I_0(k) \equiv |\psi_0|^2 = \frac{1}{R^2}$$

intensity of the object waves:

$$I_S(\mathbf{k}) \equiv |\psi_S(\mathbf{k},\mathbf{r}_j)|^2 = \frac{1}{R^2}\left|\sum_j \frac{f(\mathbf{k},\mathbf{r}_j)}{r_j^2}\right|^2$$

$I_S(\mathbf{k})/I_0 \sim 10^{-6}$ (except directions of Kossel lines)

interference between the reference and the object waves - ***hologram***:

$$\chi(\mathbf{k}) \equiv \frac{I(\mathbf{k}) - I_0}{I_0} = \frac{\psi_S^*(\mathbf{k},\mathbf{r}_j)}{\psi_0^*(\mathbf{k})} + \frac{\psi_S(\mathbf{k},\mathbf{r}_j)}{\psi_0(\mathbf{k})} \qquad \chi(\mathbf{k}) \sim 10^{-3}$$

Image reconstruction

Helmholtz-Kirchhoff integral theorem:

$$U_k(r) = \iint_{\Omega_k} \chi(\mathbf{k}) e^{-i\mathbf{k}.\mathbf{r}} d\Omega_k =$$

$$= \sum_j \left(\underbrace{\frac{e^{-ikr_j}}{r_j} \iint_{\Omega_k} f^*(\mathbf{k}.\mathbf{r}_j) e^{-i\mathbf{k}.(\mathbf{r}-\mathbf{r}_j)} d\Omega_k}_{\text{real image}} + \underbrace{\frac{e^{ikr_j}}{r_j} \iint_{\Omega_k} f(\mathbf{k}.\mathbf{r}_j) e^{-i\mathbf{k}.(\mathbf{r}+\mathbf{r}_j)} d\Omega_k}_{\text{virtual image (twin image)}} \right)$$

maxima of $|U(\mathbf{r})|$: $\mathbf{r} = \mathbf{r}_j$ $\quad$ $\mathbf{r} = -\mathbf{r}_j$

MXFH – the internal detector scheme

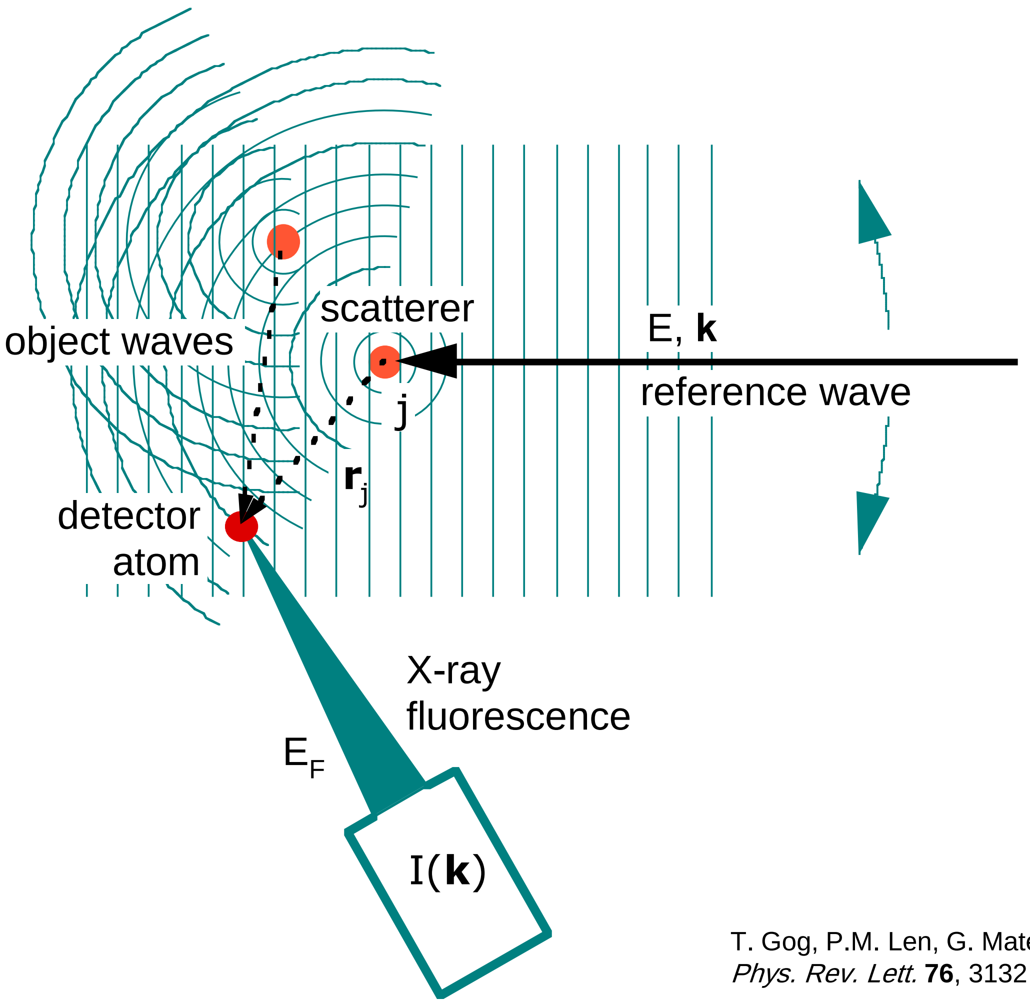

$$U(\mathbf{r}) = \sum_k U_k(\mathbf{r}) e^{-ikr}$$

T. Gog, P.M. Len, G. Materlik, D. Bahr, C.S. Fadley and C. Sanchez-Hanke
Phys. Rev. Lett. **76**, 3132 (1996).

The effect of experimental parameters

The angular region ϑ_{max} determines the resolution of the reconstructed images:

$$\Delta r = \frac{2\pi}{(k_{max} - k_{min})} = \frac{\lambda}{(1 - \cos\theta_{max})} \qquad \Delta r \geq \frac{\lambda}{2}$$

The angular resolution of the experiment $\Delta\vartheta$ determines the maximum radius r_{max} of the region around the emitter where meaningful information can be obtained:

e.g. $r_{max} = 10\,\lambda$ $\quad \Delta\theta \leq 1$ deg.

$$\Delta k << \frac{2\pi}{r_{max}}$$

$$\Delta\theta << \frac{\lambda}{r_{max}}$$

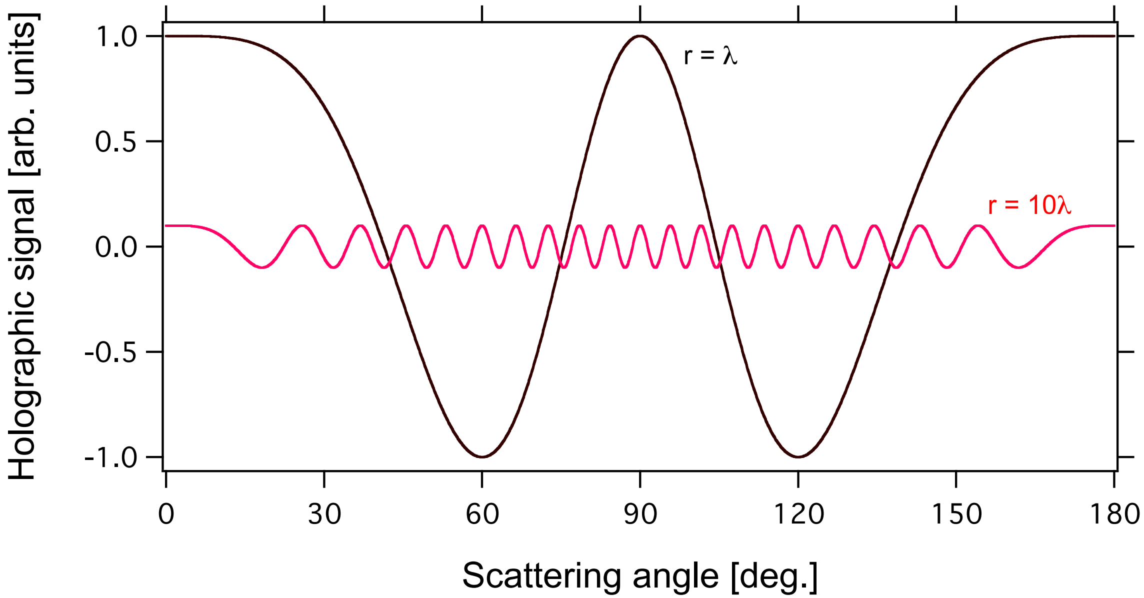

Designing the experiment

	Internal source scheme	**Internal detector scheme**
	scanning detector	scanning source

Source:

Flux	The higher the better	
Collimation	NOT REQUIRED	Low-pass filter
Monocromaticity	NOT REQUIRED	YES

Sample:

An ensemble of emitters, surrounded by an arrangement of scatteres which appears the same from whichever of the emitters it is seen.

Detector:

Energy selective	YES, to get rid of the exciting radiation scattering	
Sensitive area	Low-pass filter	TBTB
Count rate	YES	YES

experimental set-up at ELETTRA

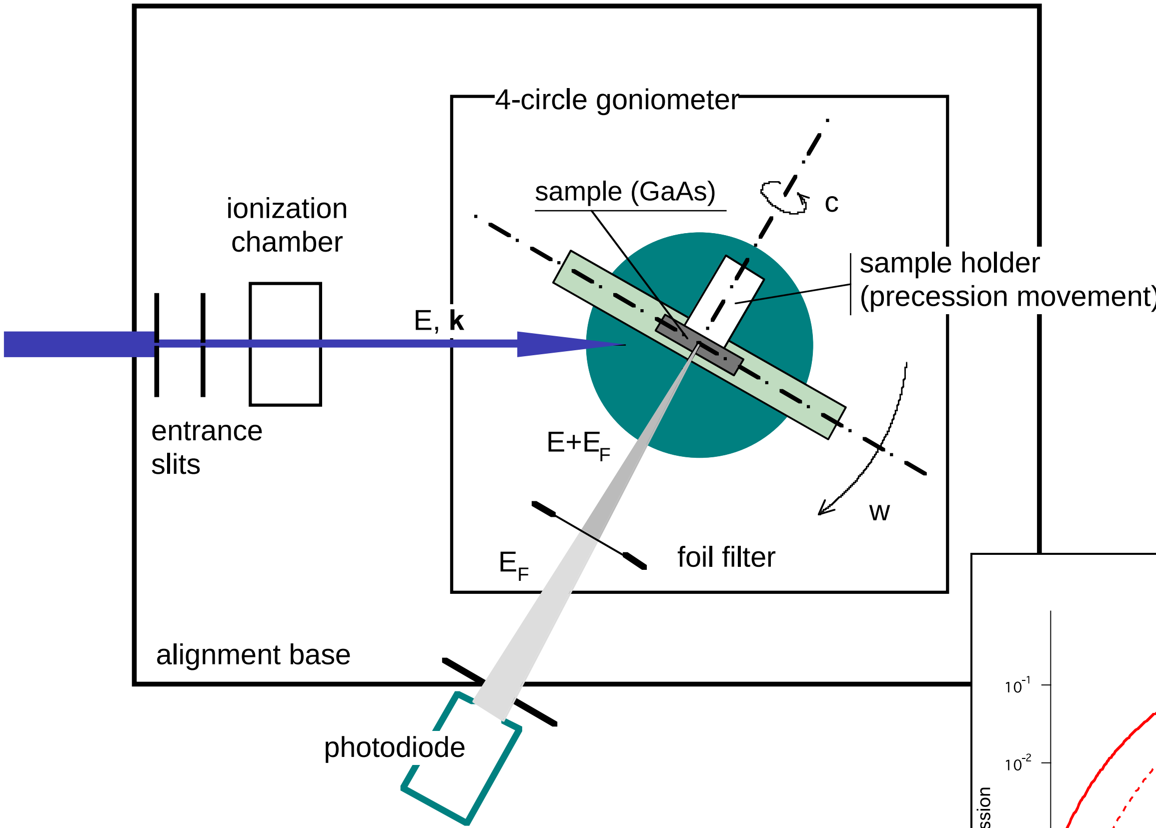

Suitable for both schemes

PIN diode

Analyser crystal
+ fast scintillation counter

Foil filter + photodiode

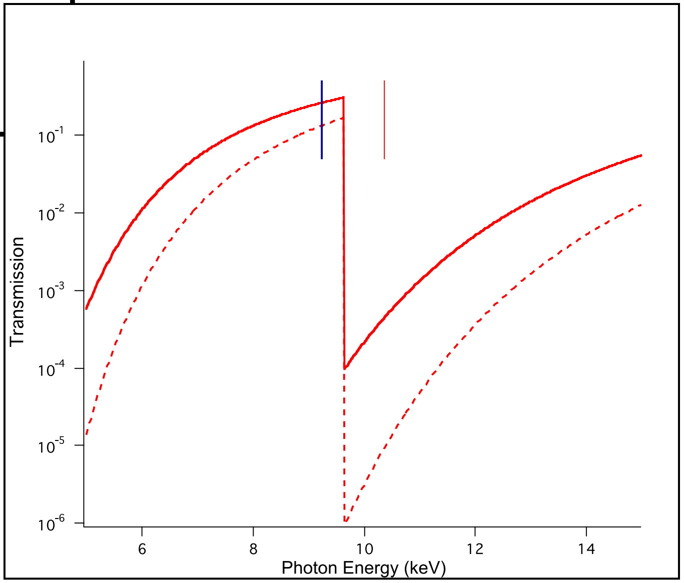

Precession Sample Holder

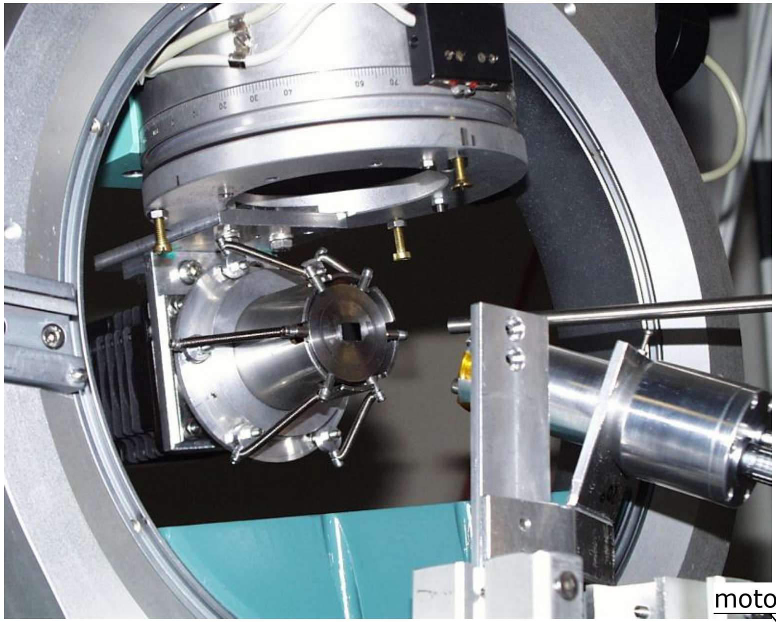

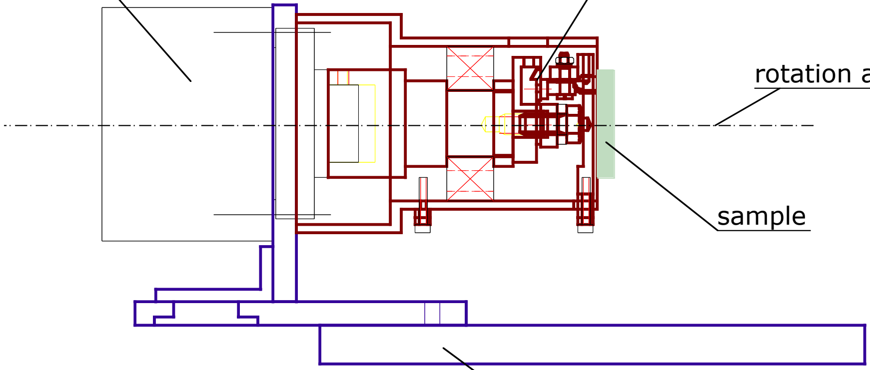

Elettra
Sincrotrone
Trieste

X ray Fluorescence Holography experiment at the ELETTRA diffraction beamline

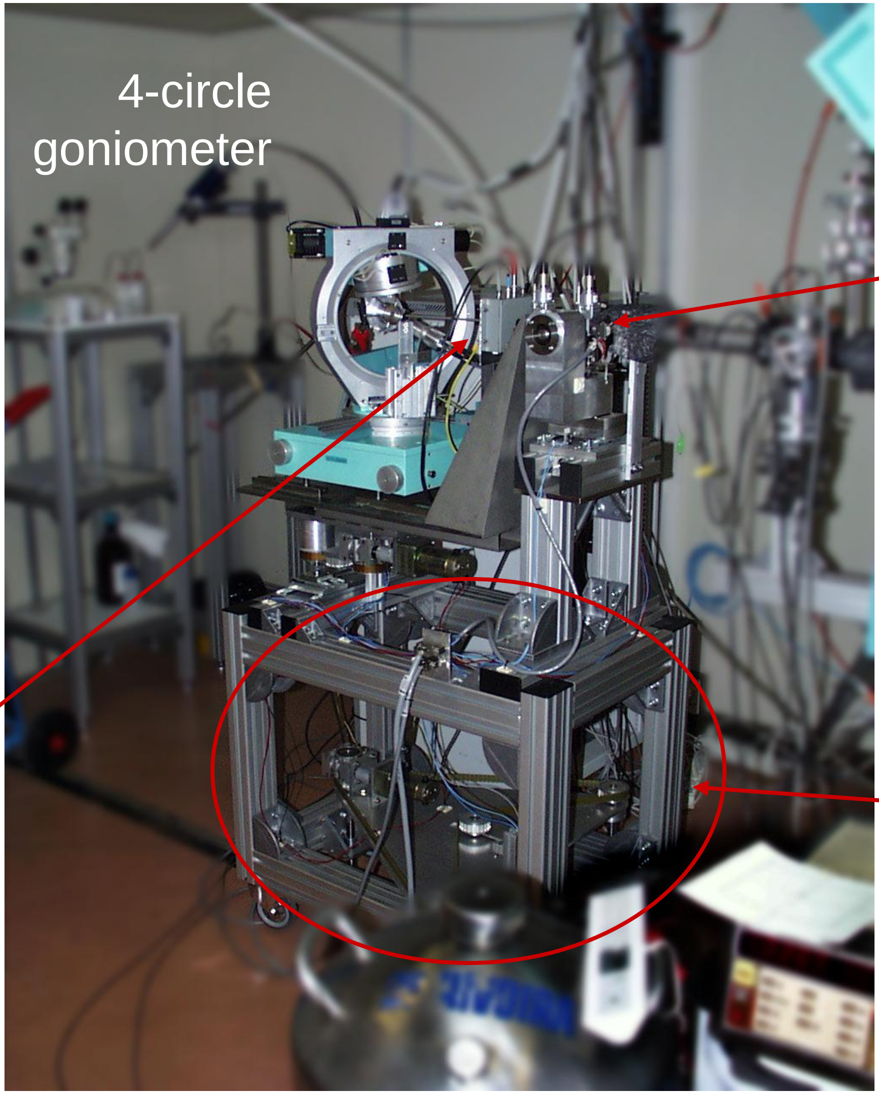

Measurement

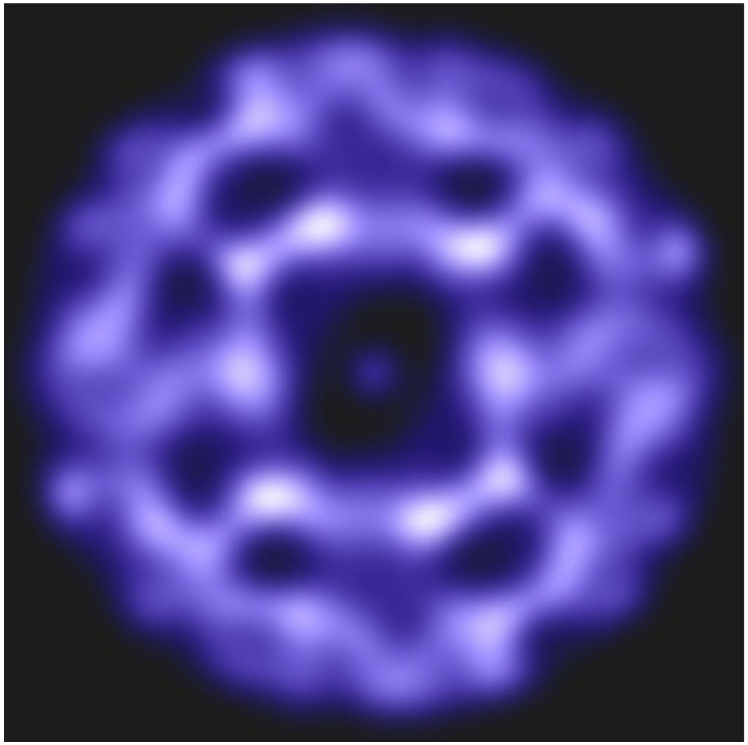

ω: [0-75 deg]; χ: [0-90 deg] $\rightarrow$ 1377 pixels
5 sec/pixel
3 hours total time
4 10^6 counts/sec per pixel

Normalization for primary beam
Low pass filter (~ 8 deg)
High pass filter

XF Hologram of GaAs

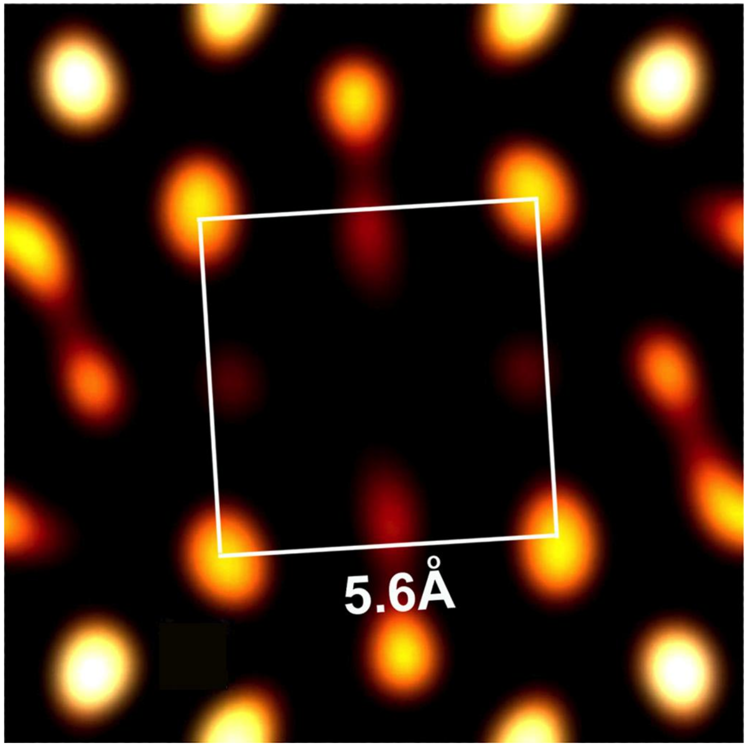

Reconstructed holographic image of GaAs(001), plane z=0

E.Busetto, M.Kopecky, A.Lausi, R. Menk, M.Miculin, and A.Savoia
Phys. Rev. **B**, **62** 5273 (2000)

Elettra
Sincrotrone
Trieste

Area detector experimental set-up

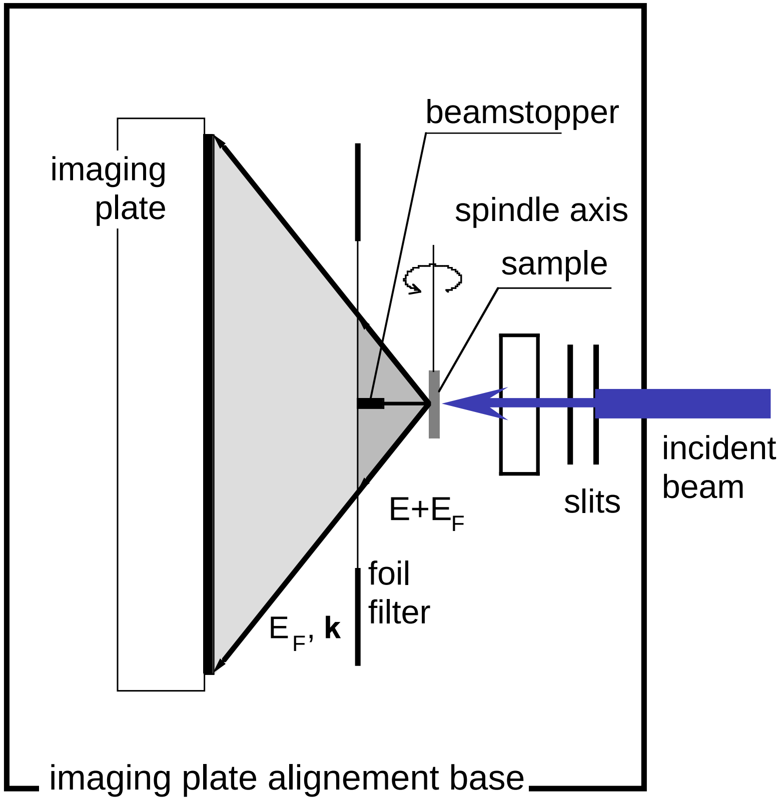

Sample size: 2 x 2 x 0.05 mm^3

Filter size: 100 x 100 mm^2

Sample-to-detector distance: 80 mm

64 images:
filter moved on a 8x8 mesh of positions with 2 mm pitch
+64 normalization images

about 3 h for 128 images

Area detector raw data

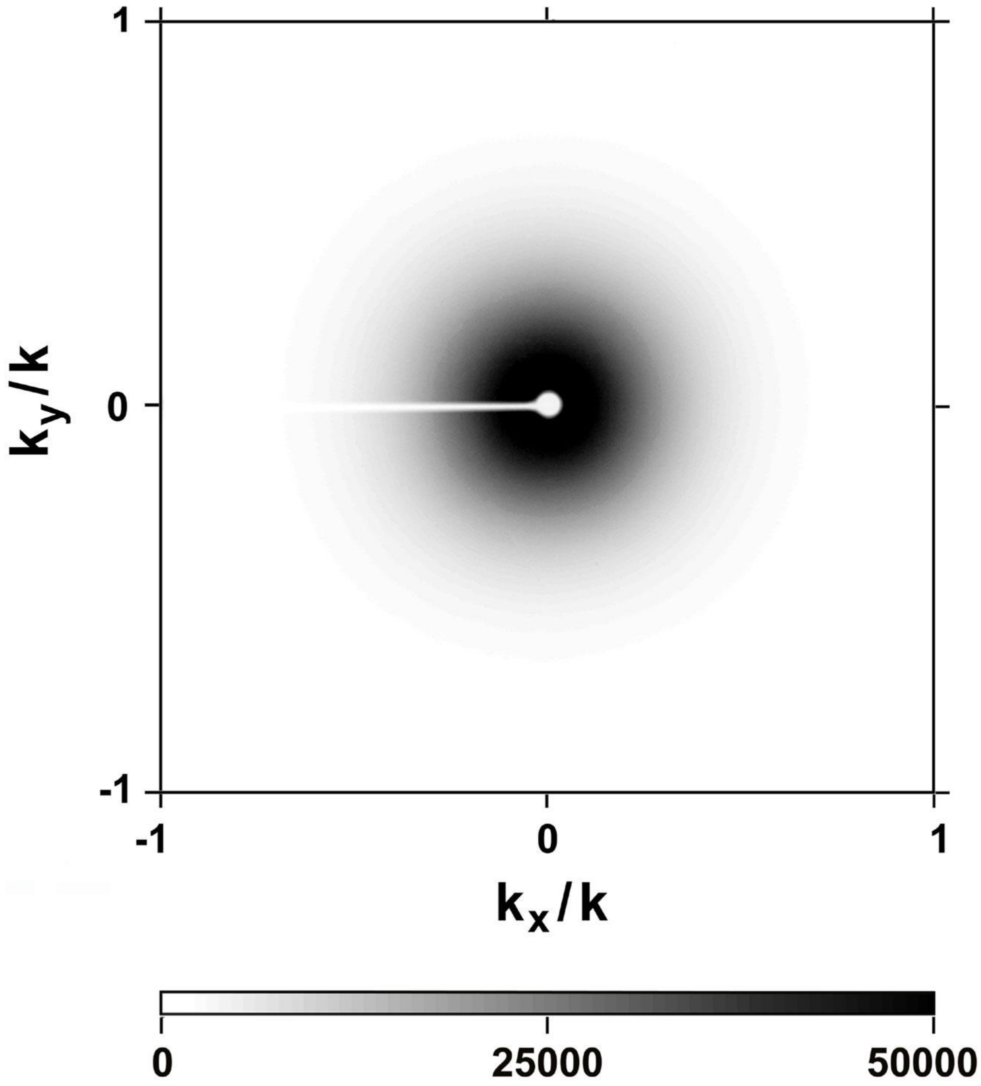

Elettra
Sincrotrone
Trieste

Area detector hologram + Kossel lines

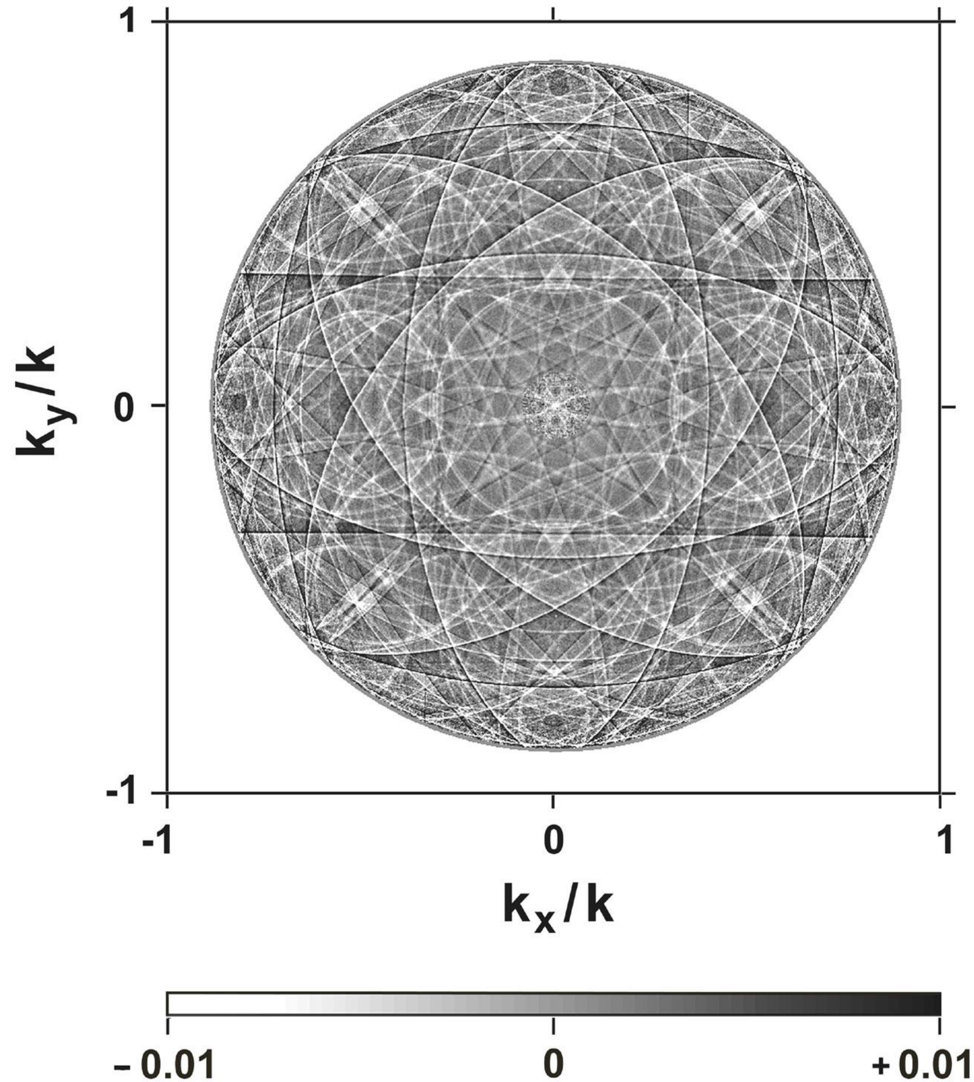

Elettra
Sincrotrone
Trieste

Area detector hologram

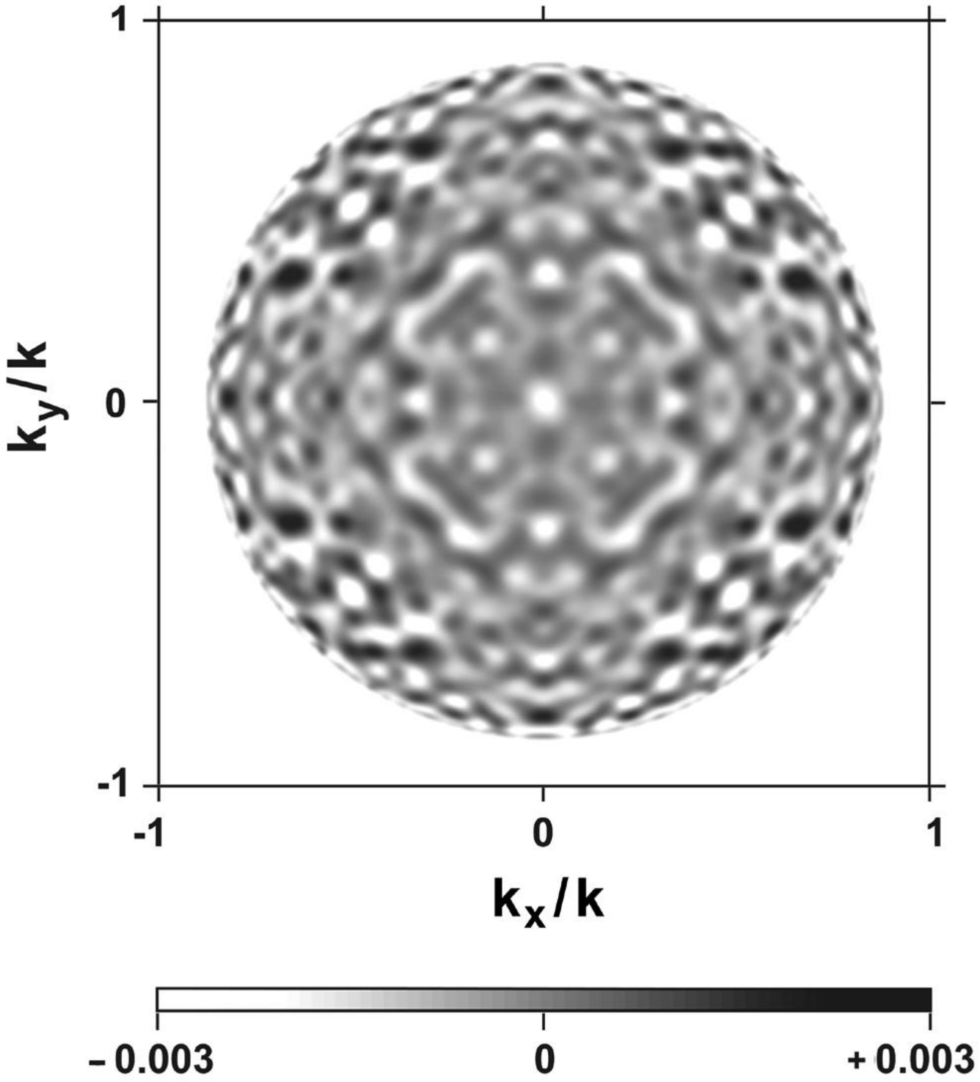

Elettra
Sincrotrone
Trieste

Area detector hologram reconstructed image

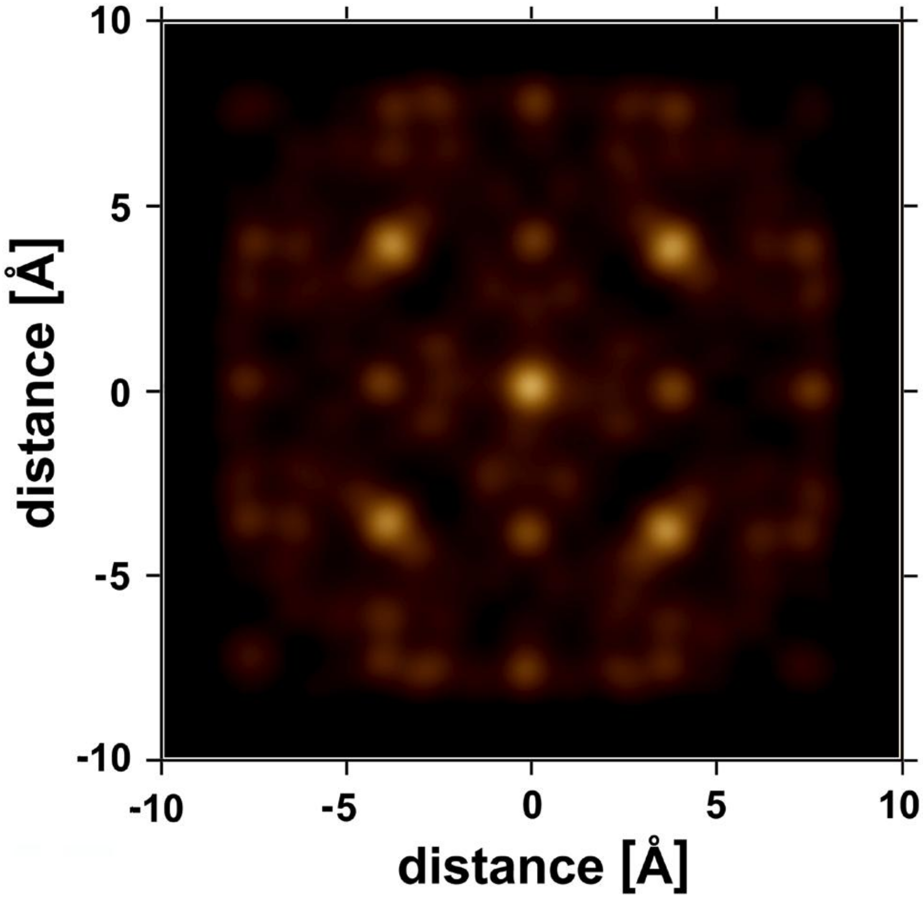

Elettra Sincrotrone Trieste

Area detector alternative experimental set-up

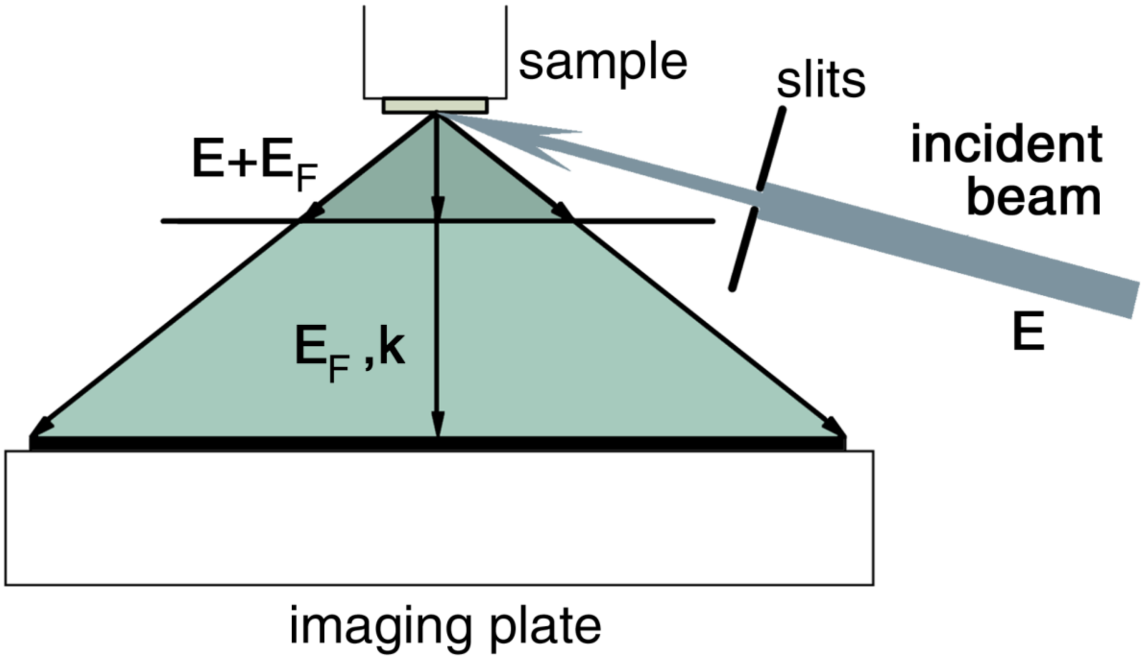

CoO sample size: 2 x 2 x 1 mm^3
Fe filter size: 100 x 100 mm^2 , 50 μm thick
E = 8.0 keV (Co K-edge @ 7.7 keV)
E_F = 6.9 keV
Sample-to-detector distance: 80 mm

Elettra
Sincrotrone
Trieste

Area detector raw data 2

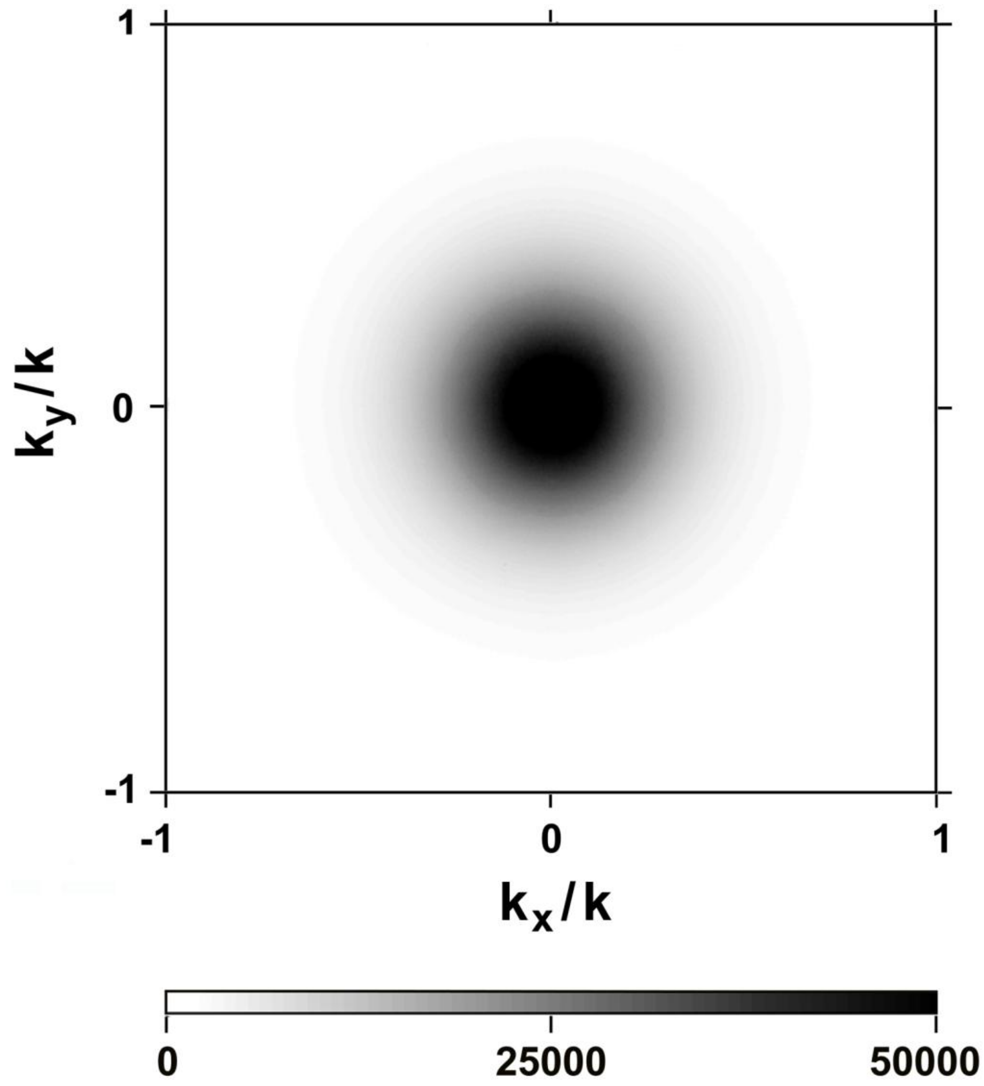

Area detector hologram + Kossel lines 2

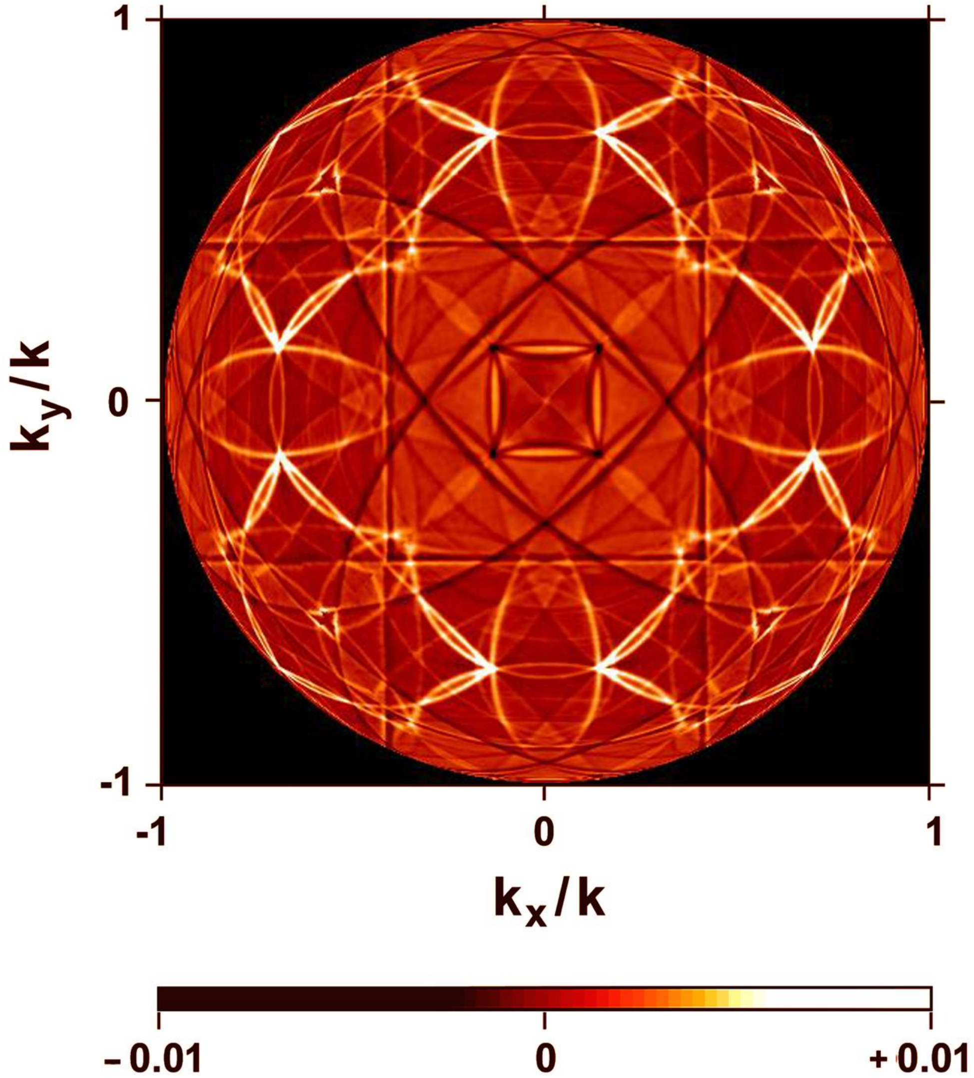

Area detector hologram 2

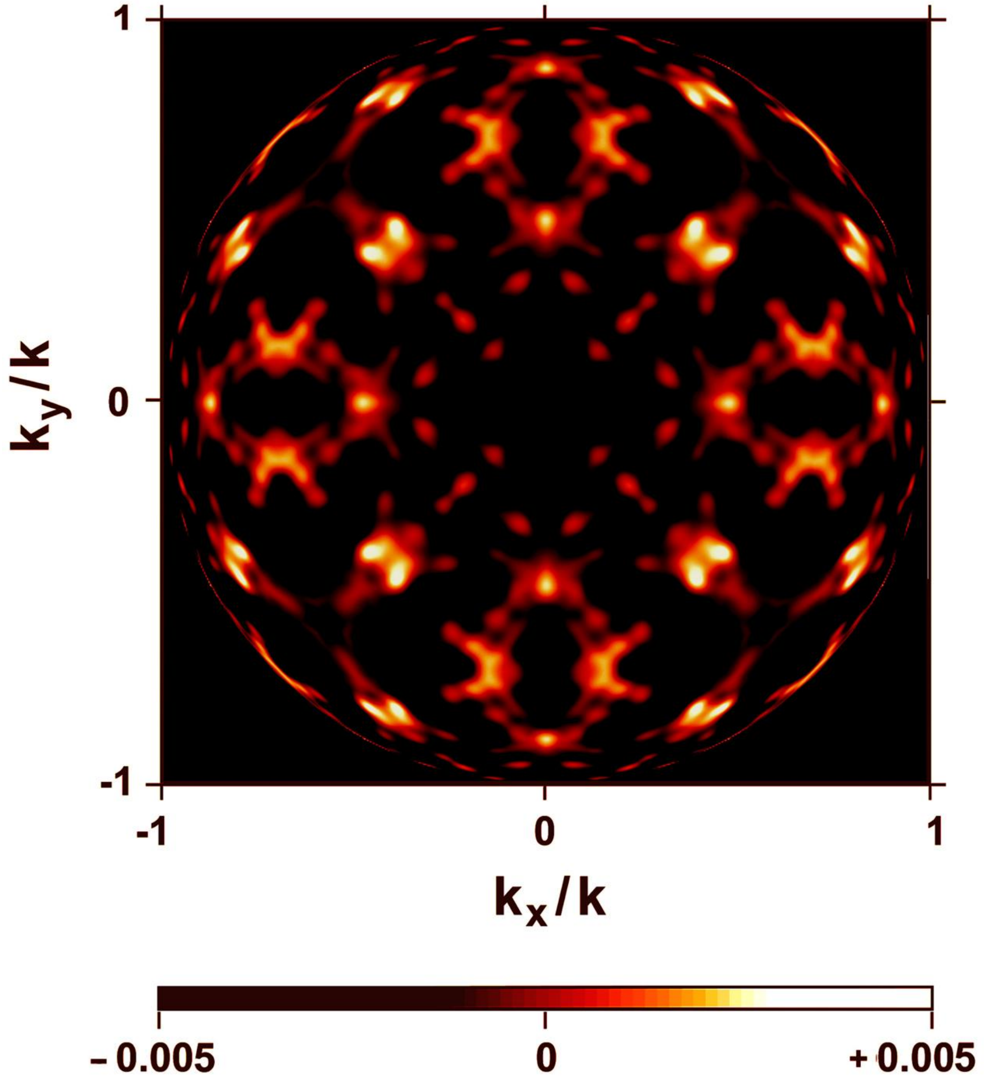

CoO hologram

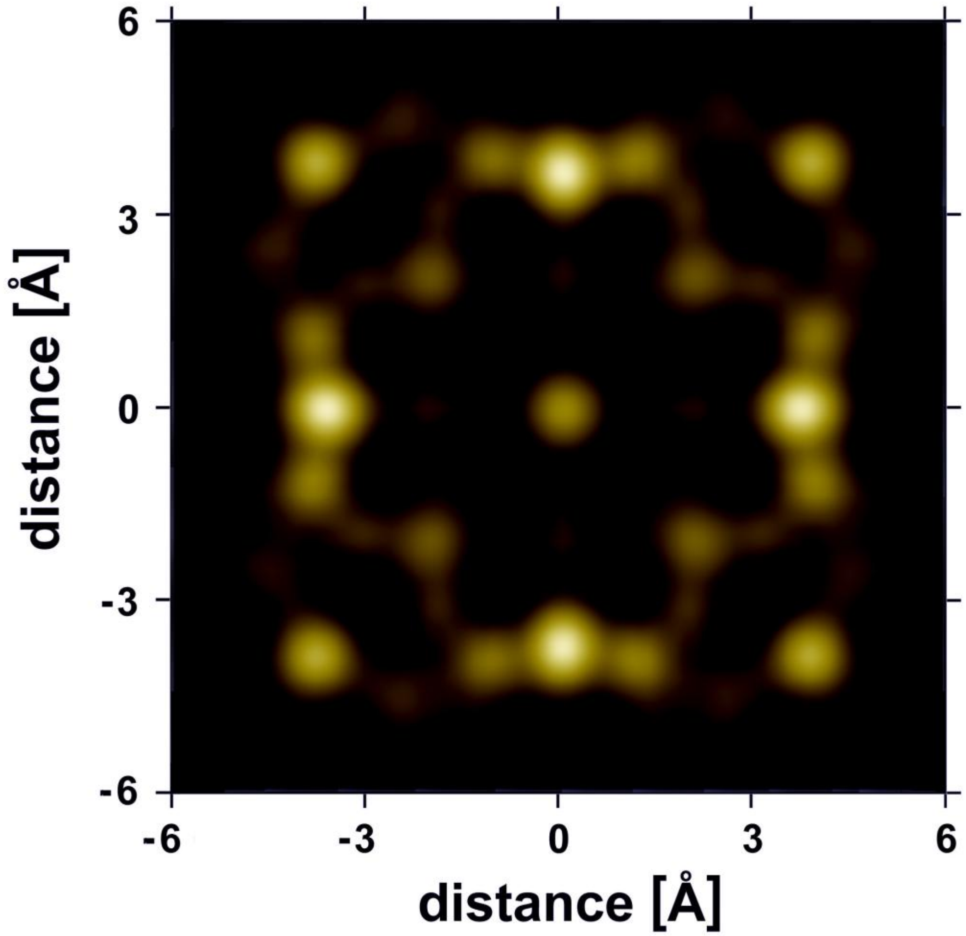

Elettra
Sincrotrone
Trieste

CoO hologram - detail

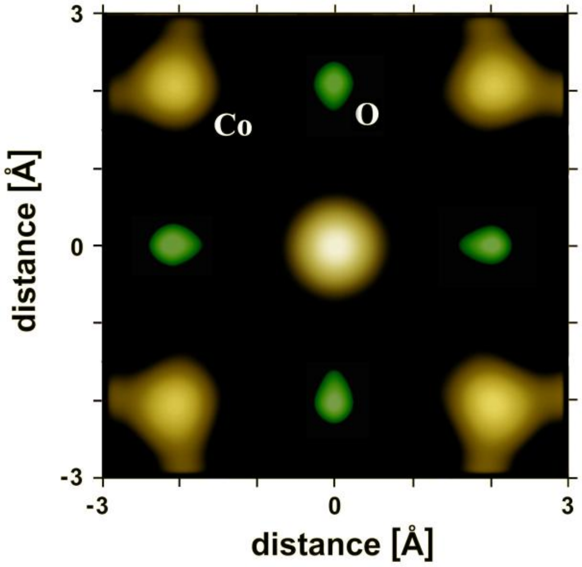

M.Kopecky, E.Busetto, A.Lausi, M.Miculin, and A.Savoia
J Appl Phys 78, 2985 (2001)

Application to diffraction pattens

Scattering from a cluster of atoms

$$I(\mathbf{k}) = \frac{I_0}{R^2} \sum_i \sum_j F_i(\mathbf{k_0}, \mathbf{k}) F_j^*(\mathbf{k_0}, \mathbf{k}) exp\left[-i(\mathbf{k} - \mathbf{k_0})(\mathbf{r}_i - \mathbf{r}_j)\right]$$

Diffraction pattern calculated for a small cluster (eight unit cells) of rock salt at an energy of 18.2 keV. The plot coordinates are defined as **k'**= **k**/k.
The incident wavevector $\mathbf{k}_0$ = (0, 0, k) is supposed to be perpendicular to a face of the unit cell; plot axes coincide with the crystallographic axes.

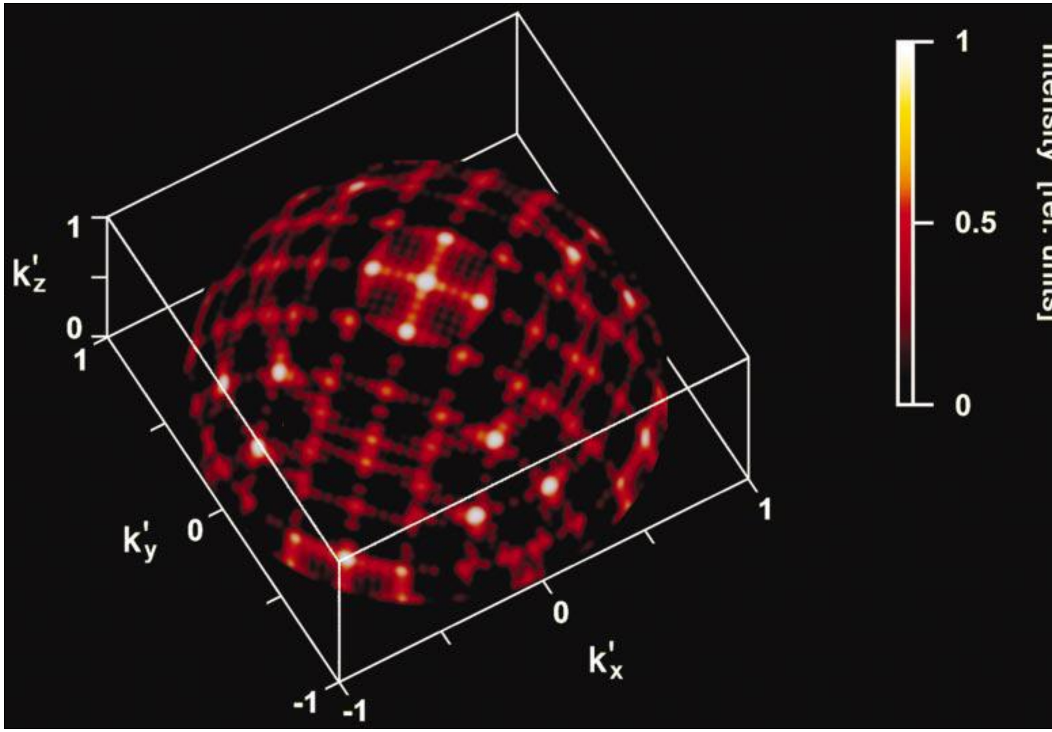

Elettra
Sincrotrone
Trieste

Real-space image

$$P(\mathbf{r}) = \int I(\mathbf{k}_0, \mathbf{k}) exp[i(\mathbf{k} - \mathbf{k}_0)\mathbf{r}] d\sigma_k = \frac{I_0}{R^2} \sum_i \sum_j F_i F_j^* \, exp[-i\mathbf{k}_0(\mathbf{r} - \mathbf{r}_{ij})] \frac{sin(k|\mathbf{r} - \mathbf{r}_{ij}|)}{k|\mathbf{r} - \mathbf{r}_{ij}|}$$

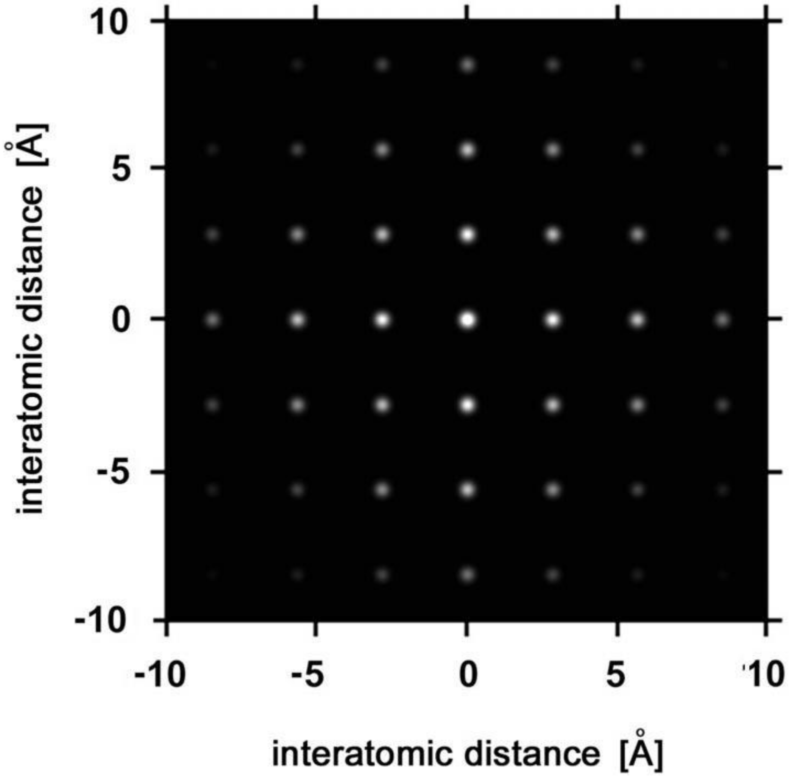

The function P(r) in the plane z = 0 obtained from the simulated diffraction pattern. The positions of local maxima coincide with interatomic distances.

Elettra
Sincrotrone
Trieste

Test: diffuse scattering from crystal

Diffuse X-ray scattering from an NaCl crystal recorded on a CCD detector.

Photon energy 18.2 keV. Sample surface in the xy plane oriented perpendicular to the incident beam with a wavevector $k_0 = (0, 0, k)$.

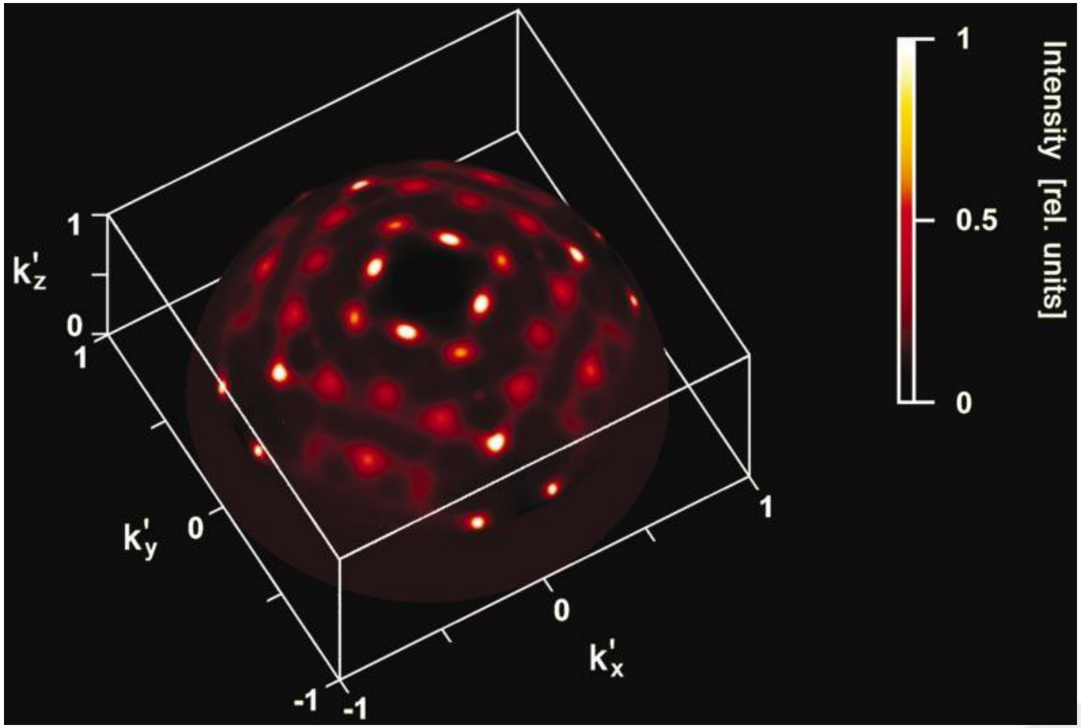

Diffuse scattering reconstruction

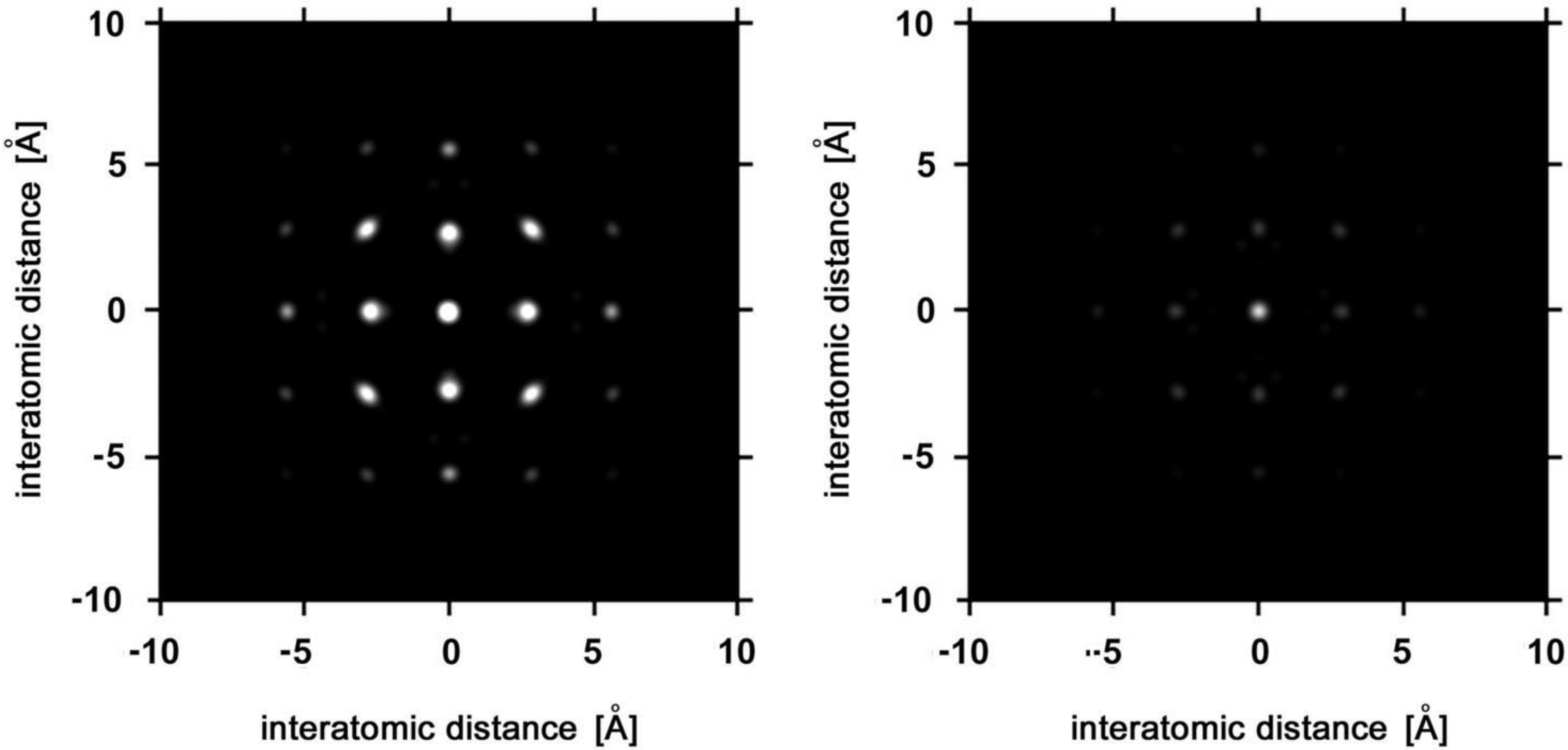

X-Ray Diffuse Scattering Holography - theory

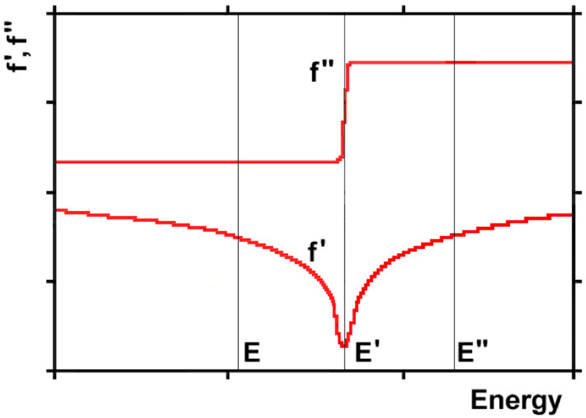

$$f_i^{E'} = f_i^{E} \equiv f_i \qquad i \neq n$$

$$f_n^{E'} = f_n^{E} + \Delta f_n \equiv f_n + \Delta f_n$$

$$\Delta f_n = \Delta f_n{}' + \Delta f_n{}''$$

INTENSITY:

$$I(\mathbf{k},\mathbf{k}_0) = \frac{I_0}{R^2}\sum_{i=1}^{N}\sum_{j=1}^{N} f_i(\mathbf{k},\mathbf{k}_0) f_j^*(\mathbf{k},\mathbf{k}_0) e^{-i(\mathbf{k}-\mathbf{k}_0)(\mathbf{r}_i-\mathbf{r}_j)}$$

$$I(\mathbf{k}',\mathbf{k}'_0) = \frac{I_0}{R^2}\left(\Delta f_n e^{-i(\mathbf{k}'-\mathbf{k}'_0).\mathbf{r}_n} + \sum_i f_i e^{-i(\mathbf{k}'-\mathbf{k}'_0).\mathbf{r}_i}\right) \times$$

$$\times\left(\Delta f_n^* e^{i(\mathbf{k}'-\mathbf{k}'_0).\mathbf{r}_n} + \sum_j f_j^* e^{i(\mathbf{k}'-\mathbf{k}'_0).\mathbf{r}_j}\right)$$

If $(\Delta\mathbf{k} - \Delta\mathbf{k}_0)\cdot\mathbf{r}_i \to 0$ **and** $\mathbf{r}_n$ ° $(0,0,0)$

$$\chi(\mathbf{k},\mathbf{k}_0) = I(\mathbf{k}',\mathbf{k}'_0) - I(\mathbf{k},\mathbf{k}_0) =$$

$$= \frac{I_0}{R^2}\left(\Delta f_n^* \sum_j f_j e^{-i(\mathbf{k}-\mathbf{k}_0).\mathbf{r}_j} + \Delta f_n \sum_j f_j^* e^{i(\mathbf{k}-\mathbf{k}_0).\mathbf{r}_j} + \Delta f_n \Delta f_n^*\right)$$

(Kopecký M.: J. Appl. Cryst. 37, (2004), 711)

X-Ray Diffuse Scattering Holography - theory, continued

IMAGE RECONSTRUCTION:

$$U(\mathbf{r}) = \frac{R^2}{I_0} \int_{\Omega_k} \Delta I(\mathbf{k},\mathbf{k}_0) e^{i(\mathbf{k}-\mathbf{k}_0).\mathbf{r}} \mathbf{dk}$$

$$U(\mathbf{r}) = \Delta f_n^* \sum_j \int_{\Omega_k} f_j e^{-i(\mathbf{k}-\mathbf{k}_0).(\mathbf{r}_j-\mathbf{r})} \mathbf{dk} + \Delta f_n \sum_j \int_{\Omega_k} f_j^* e^{i(\mathbf{k}-\mathbf{k}_0).(\mathbf{r}_j+\mathbf{r})} \mathbf{dk} +$$

***real image** at $\boldsymbol{r} = \boldsymbol{r}_j$* ***virtual image** at $\boldsymbol{r} = -\boldsymbol{r}_j$*

$$+ \int_{\Omega_k} \left|\Delta f_n\right|^2 e^{i(\mathbf{k}-\mathbf{k}_0).\mathbf{r}} \mathbf{dk}$$

(Kopecký M.: J. Appl. Cryst. 37, (2004), 711)

X-Ray Diffuse Scattering Holography - data

Diffraction patterns **Hologram**

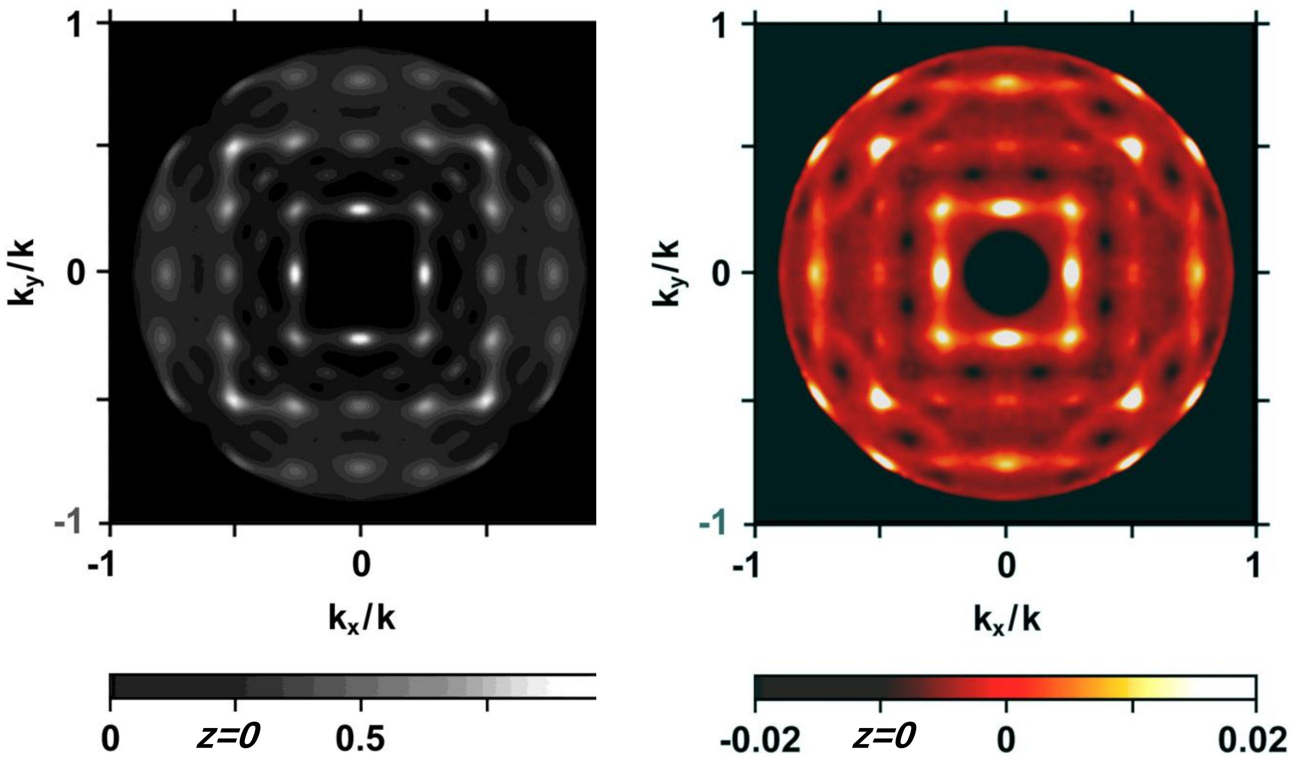

Rubidium Chloride *E = 15.06 keV, ⊗E = 60 eV*

(Kopecký et al., Appl. Phys. Lett. 87 (2005), 2319

X-Ray Diffuse Scattering Holography - reconstruction

Pair distribution function

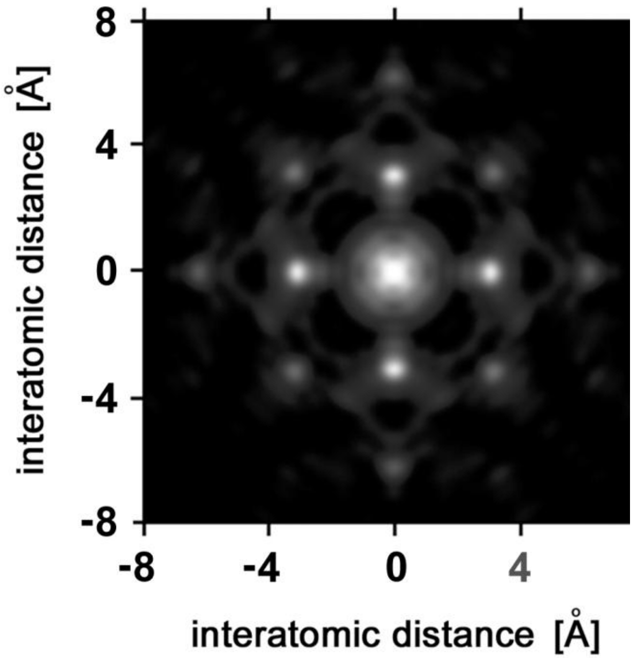

z=0

Electron density

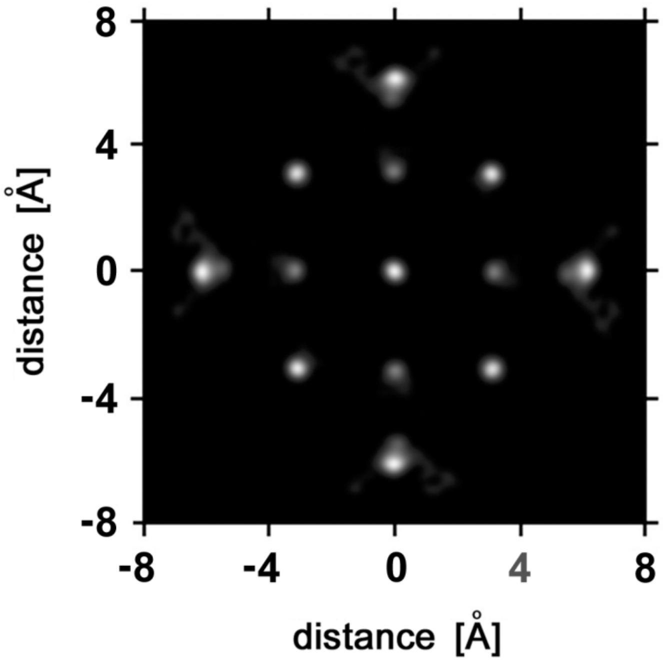

z=0

Elettra
Sincrotrone
Trieste

(Kopecký et al., Appl. Phys. Lett. 87 (2005), 231914)

GaMnAs layers

= diluted magnetic semiconductor (magnetic and semiconducting properties) promising for spin electronics

Magnetic properties (e.g. Curie temperature T_C) are strongly related to Mn sites:

Mn in ***substitutional position*** act as an ***acceptor*** and created a hole

Mn in ***interstitial position*** acts as a ***double donor*** and passivates two holes

c-RBS and c-PIXE (channeling Rutherford backscattering and particle induced x-ray emission

- presence of interstitials can be verified

Indirect methods

Concentration of interstitial atoms is often estimated by comparing experimental data with theoretical models using:

- changes of a lattice parameter due to interstitial atoms
- integral intensities of weak Bragg reflections

XFH (x-ray fluorescence holography)

a three-dimensional atomic image around Mn atoms in $Zn_{0.4}Mn_{0.6}Te$

application to very thin $Ga_{1-x}Mn_xAs$ layers with low concentration of dopants ($x < 0.1$) is problematic because of the weak fluorescence signal

XDSH (x-ray diffuse scattering holography)

a three-dimensional atomic image around Mn atoms in GaMnAs

GaMnAs layers -Experimental Configuration

- ❖material science beamline ID11 at the European Synchrotron Radiation Facility in Grenoble, France (J. P. Wright)
- ❖GaMnAs layers grown by low-temperature MBE, Institute of Physics, Prague (M. Cukr, V. Novák, K. Olejník)
- ❖photon energy 30 keV
- ❖conditions of total reflection (grazing angle of 0.07°)
- ❖beam size 300 μm (horizontal) × 10 μm (vertical)
- ❖16-bit CCD camera
- ❖FreLon2k16 (2048 × 2048 pixels, pixel size 46 × 46 μm^2)
- ❖sample-to-detector distance 65 mm
- ❖exposure time 20 s per frame

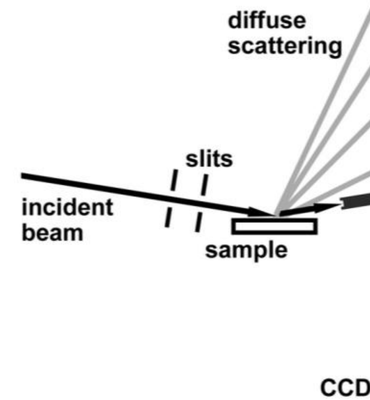

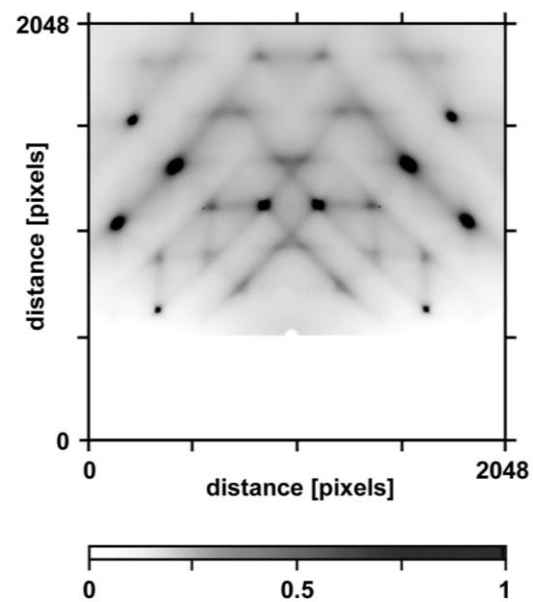

$GaMn_xAs$ layers at lower concentration of Mn: x = 0.02

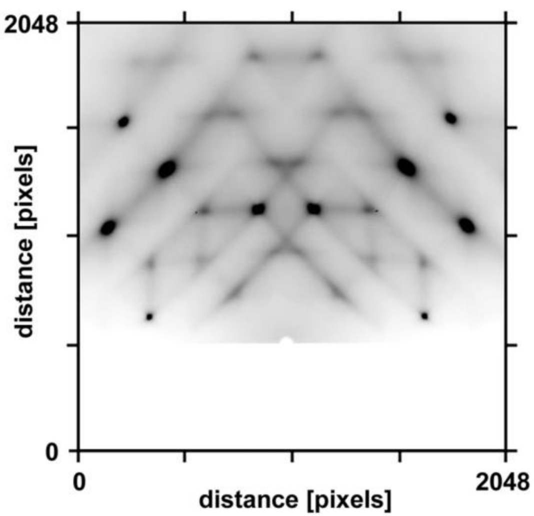

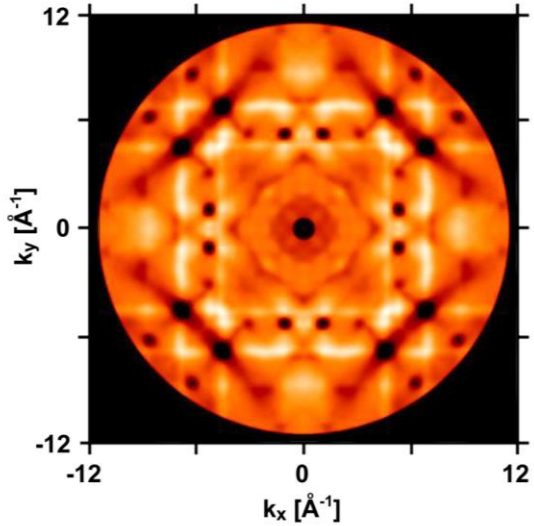

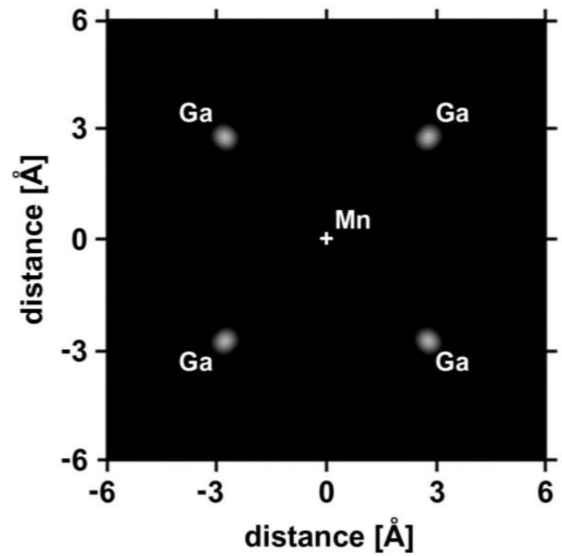

Reconstruction algorithm

= local neighborhood of dopants

Diffraction patterns → **Hologram** → **Electron density**

Mn atoms in

SUBSTITUTIONAL POSITIONS

isomorphous replacement

GaMnAs

×

GaAs

Elettra Sincrotrone Trieste

(Kopecký et al., J. Appl. Cryst. 39 (2006), 735)

X-Ray Diffuse Scattering Holography - advantages

Overcomes experimental difficulties:

X-ray fluorescence holography

- low signal-to-background ratio (~ 0.1 %)
- intense and dense Kossel line patterns
- virtual images

solved by XDSH

- signal-to-background ratio 1-10 %
- discrete (and thus removable) Bragg peaks instead of Kossel lines
- virtual images can be removed by measuring a complex hologram (for centrosymmetric samples, virtual image = real image)

Fundamental problem:

- wavelength of x rays of the same order as interatomic distances

=> ***strong artefacts*** in the reconstructed image

solved by multi-energy anomalous diffuse scattering (MADS)

Multi-Energy Anomalous Diffuse Scattering

XDSH **vs** **MADS**

intensities measured at

TWO-DIMENSIONAL surface | **THREE-DIMENSIONAL** region

in the reciprocal space

reconstructed real-space-image

STRONG ARTEFACTS | **FREE OF ARTEFACTS**

MADS extends principles of XDSH to three dimensions

(Kopecký M., Fábry J., Kub J., Lausi A., Busetto E.: Phys. Rev. Lett. 100 (2008), 195504)

Multi-Energy Anomalous Diffuse Scattering

MAD	vs	MADS
	intensities measured in	
DISCRETE POINTS (Bragg peaks)		CONTINUOUS REGION (diffuse scattering)
	in the reciprocal space	
	⇩	
	provides information on	
LONG-RANGE ORDERING		SHORT-RANGE ORDERING

MADS applies principles of MAD to diffuse scattering

(Kopecký M., Fábry J., Kub J., Lausi A., Busetto E.: Phys. Rev. Lett. 100 (2008), 195504)

Multi-Energy Anomalous Diffuse Scattering

Three-dimensional pattern of diffuse scattering intensity of a $SrTiO_3$ single crystal collected at the photon energy of 14 keV

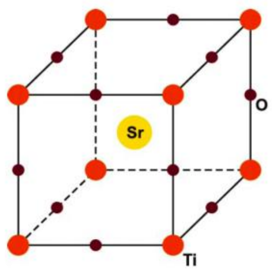

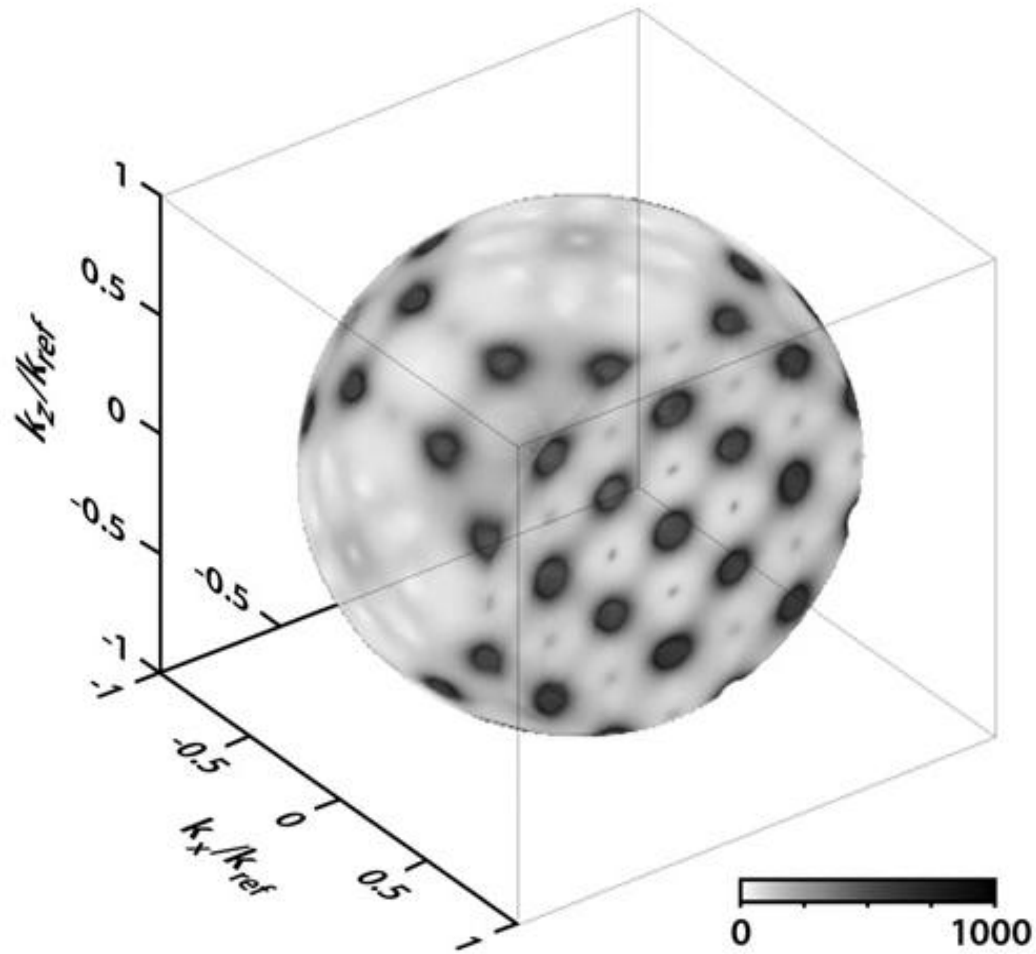

Elettra
Sincrotrone
Trieste

Multi-Energy Anomalous Diffuse Scattering

The anomalous diffuse scattering pattern

obtained as a difference of two diffuse scattering patterns

recorded at energies of 14 keV and 16.055 keV

(i.e. 50 eV below the K absorption edge of strontium)

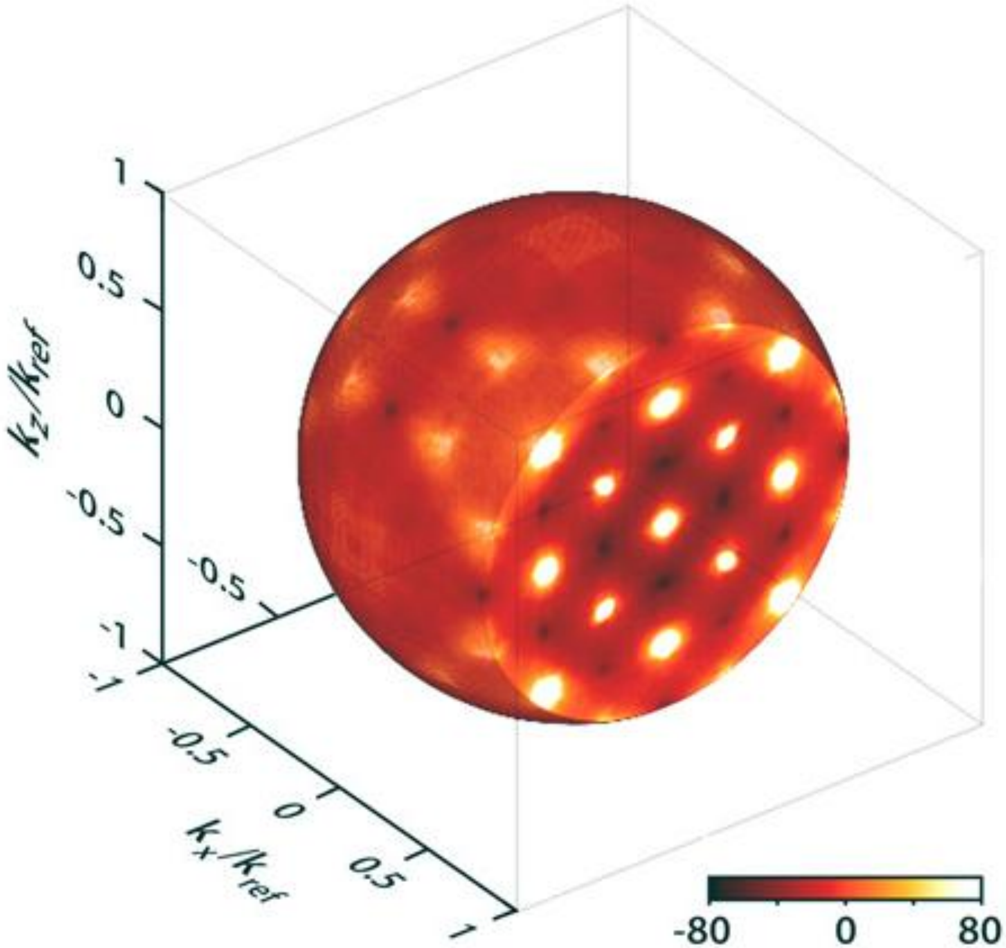

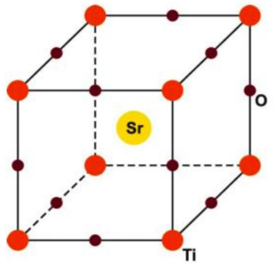

Elettra
Sincrotrone
Trieste

Multi-Energy Anomalous Diffuse Scattering

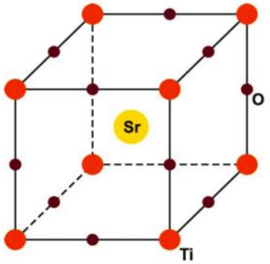

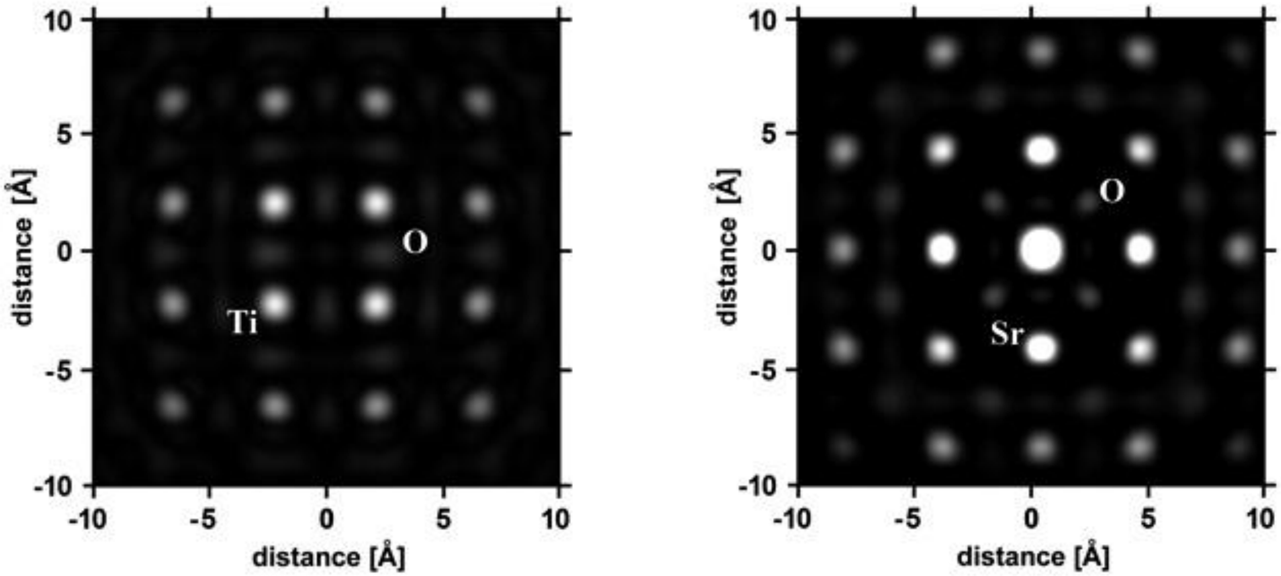

Reconstructed image of the atomic planes parallel to the (001) crystallographic plane at *z = a* and *z = 3a/2* (*a* = 3.905 Å)

Thanks…

M. KOPECKÝ, J. FÁBRY, J. KUB, Z. ŠOUREK *Institute of Physics of AS CR, Prague, Czech Republic*
E. BUSETTO *Sincrotrone Trieste, Italy*
J. P. WRIGHT *ESRF, Grenoble, France*

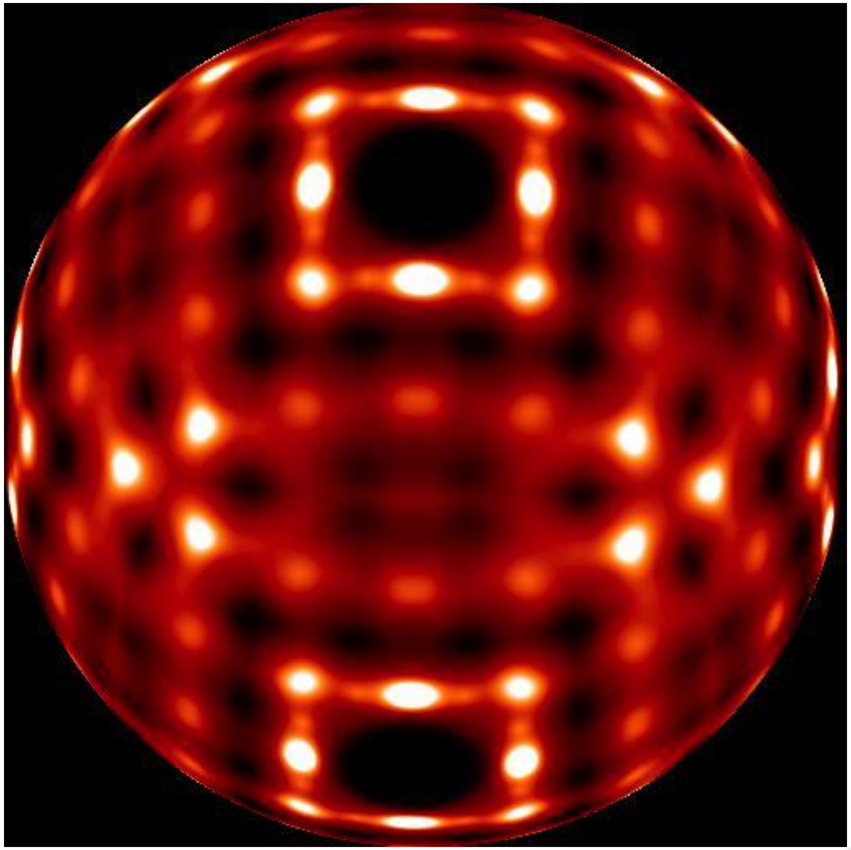

M Kopecký
J Kub

Institute of Physics, Academy of Sciences of the Czech Republic

E Busetto

ELETTRA

Elettra
Sincrotrone
Trieste